How wet are slabs : Studying the link between slab low velocity structures and intermediate depth seismicity

Andreas Rietbrock

Sebastian Martin, Tom Garth, Sophie Coulson

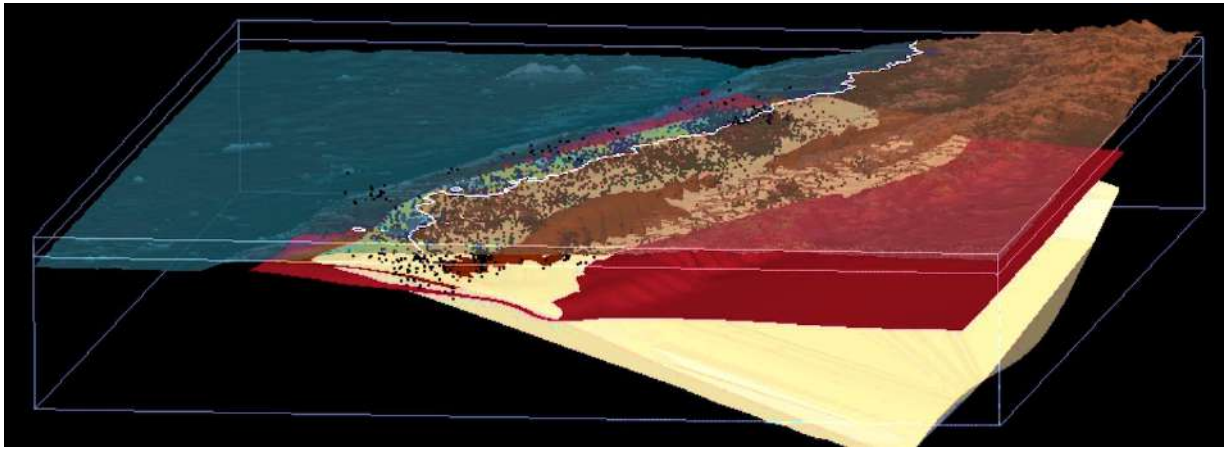

S. Hicks

Wadati-Benioff-Zone seismicity

Figure 5.4-22: Model for intermediate-depth earthquakes.

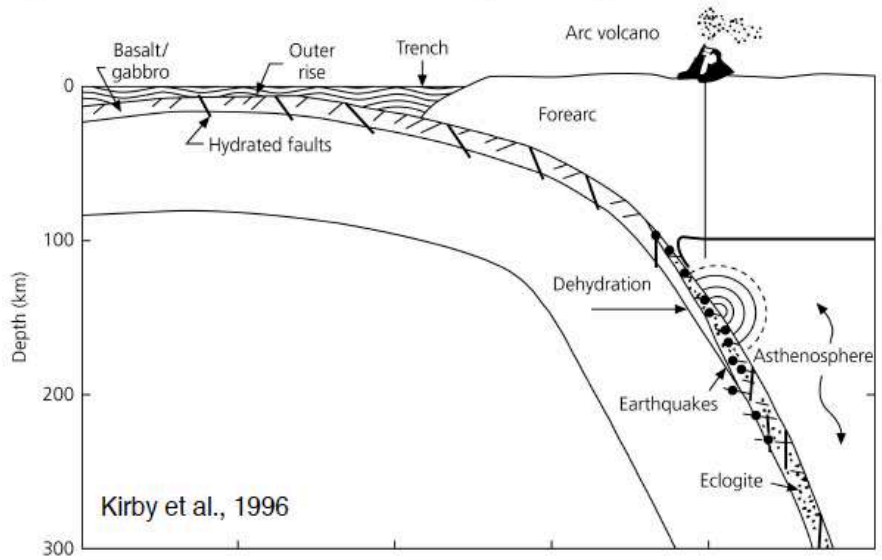

Chile

Japan

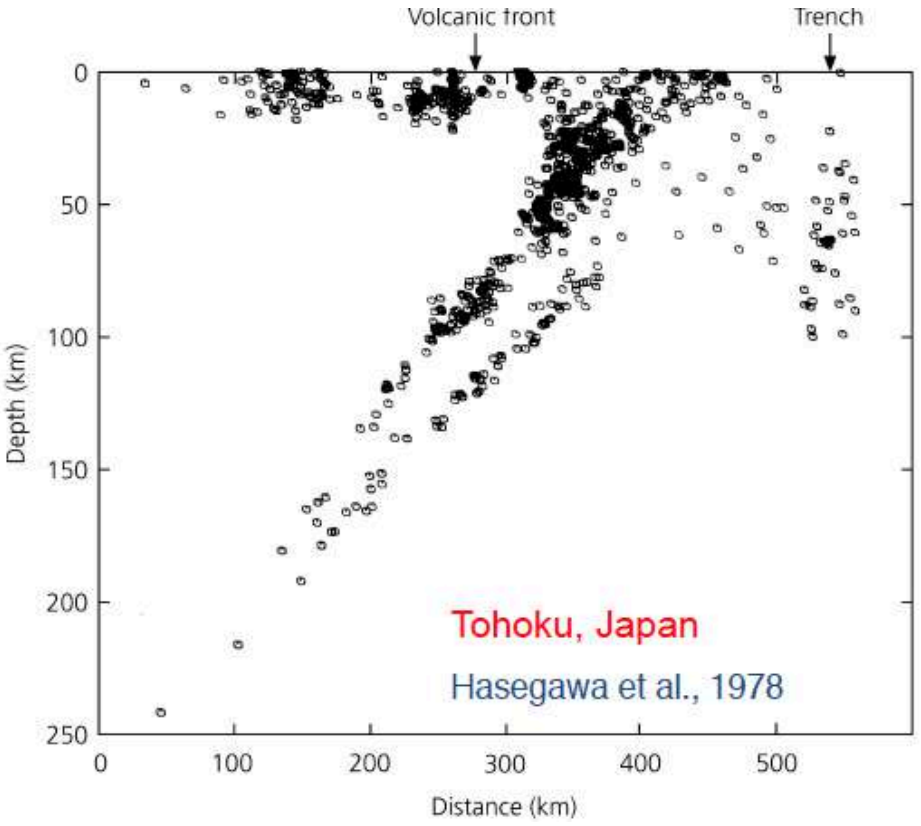

Fine structure of intermediate depth seismicity

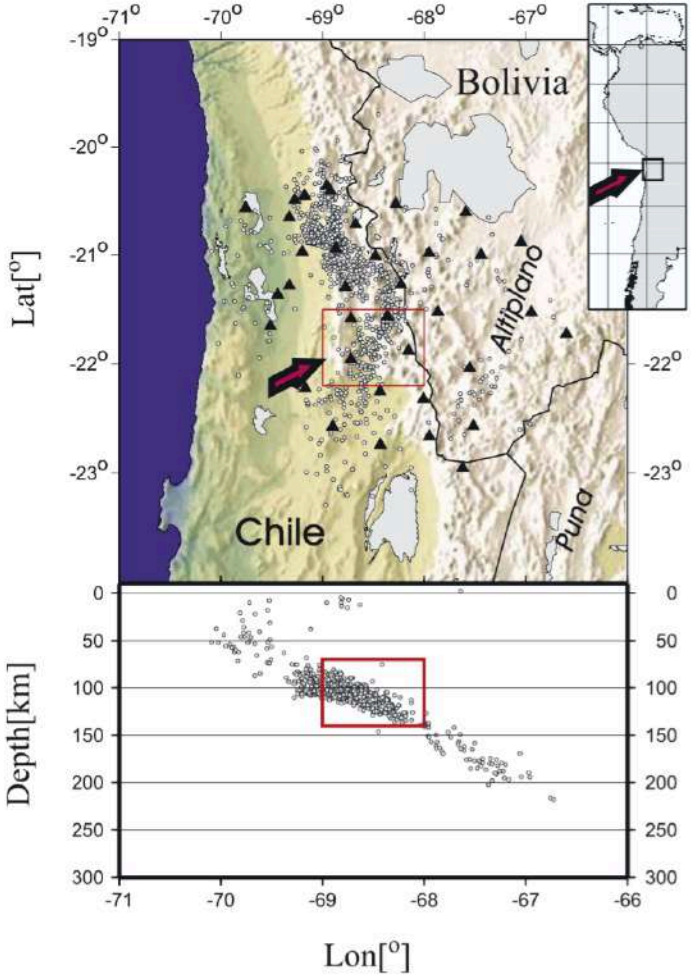

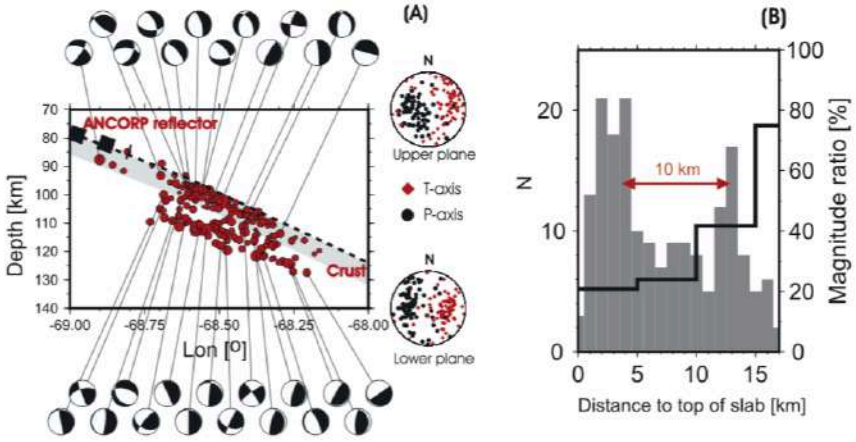

Figure 3. (a) Relocated seismicity of Figure 2) and fault plane solutions based on first-motion polarities (lower hemisphere projection). Individual mechanisms are shown for events with magnitude $M_L > 2.5$. P-axes (pressure) and T-axes (extension) are shown in a combined stereographic plot for both the upper and lower band seismicity. Superimposed on the seismicity is the thickness of the oceanic crust as derived from offshore refraction profiles [*Patzwahl et al.*, 1999]. The top of the Nazca plate (dashed line) is inferred from steep-angle reflection profiles to the north [*ANCORP Working Group*, 1999] and south [*Yoon et al.*, 2003]. (b) Depth distribution of the relocated events with respect to the top of the Nazca plate (gray bars) and

Rietbrock&Waldhauser (2004)

Double Wadati-Benioff-Zone (WBZ) in young slabs

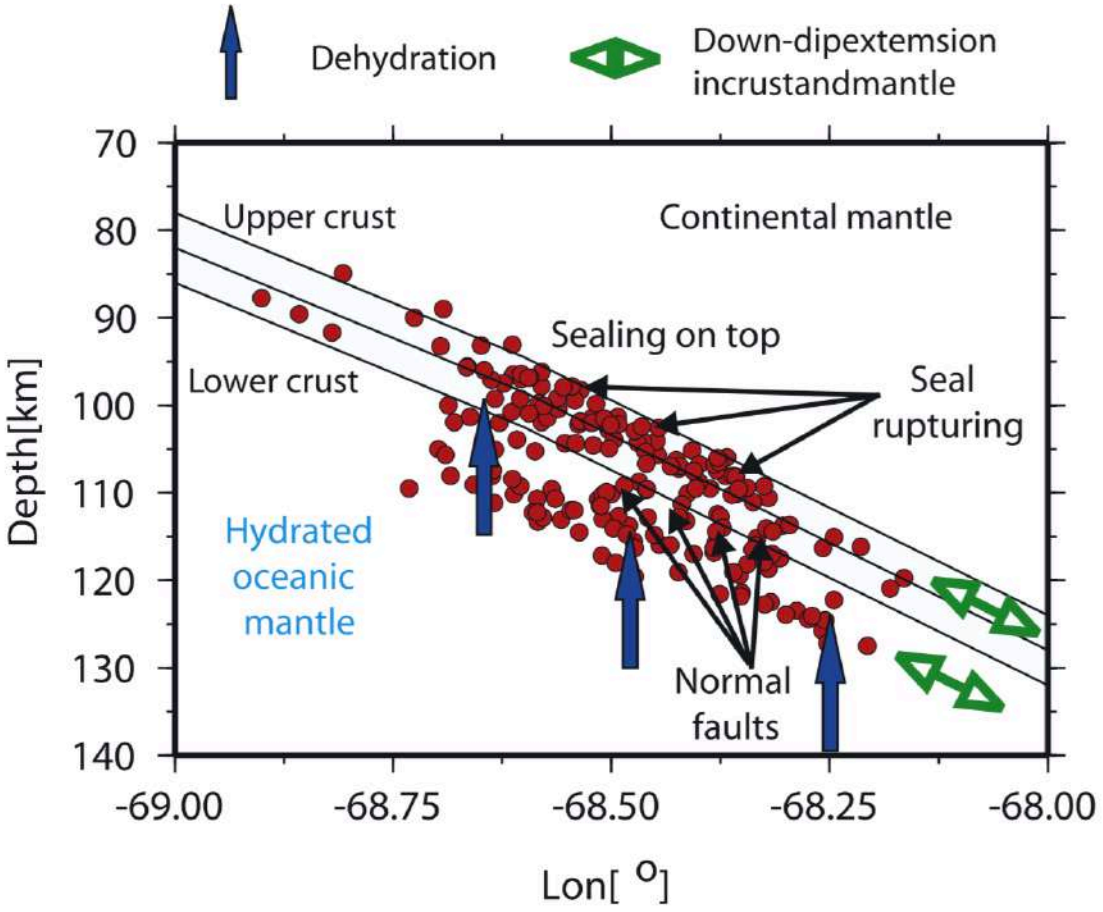

Rietbrock&Waldhauser (2004)

Global Prevalence of DWBZ

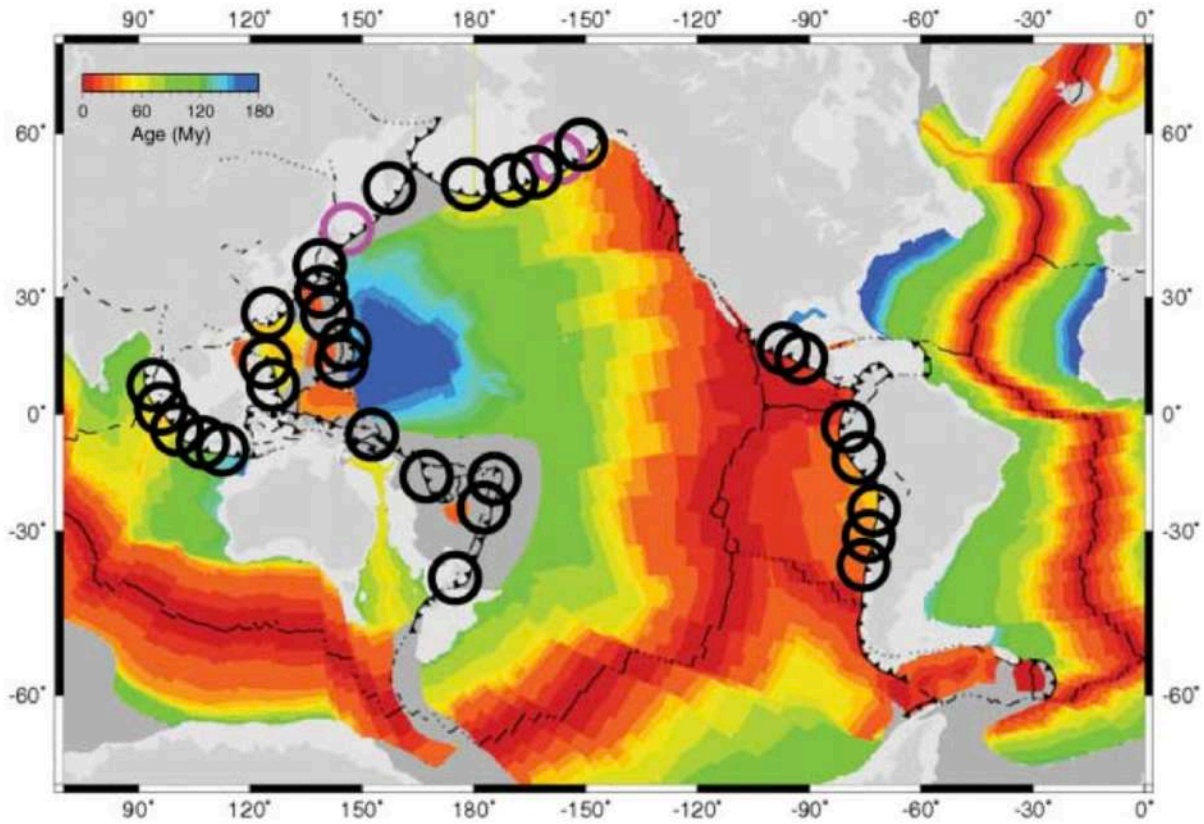

Fig. 1. Subduction-zone segments analyzed, with color scale illustrating seafloor age (*28*) before being consumed at trenches (barbed lines). Black circles indicate areas with a multimodal distribution of events in the slab-normal direction (pink circles indicate cases with confidence < 95%), demonstrating that DBZs are globally prevalent.

Brudzinsky et al. (2007)

Global earthquake catalogues show on average a clear signal for DWBZs

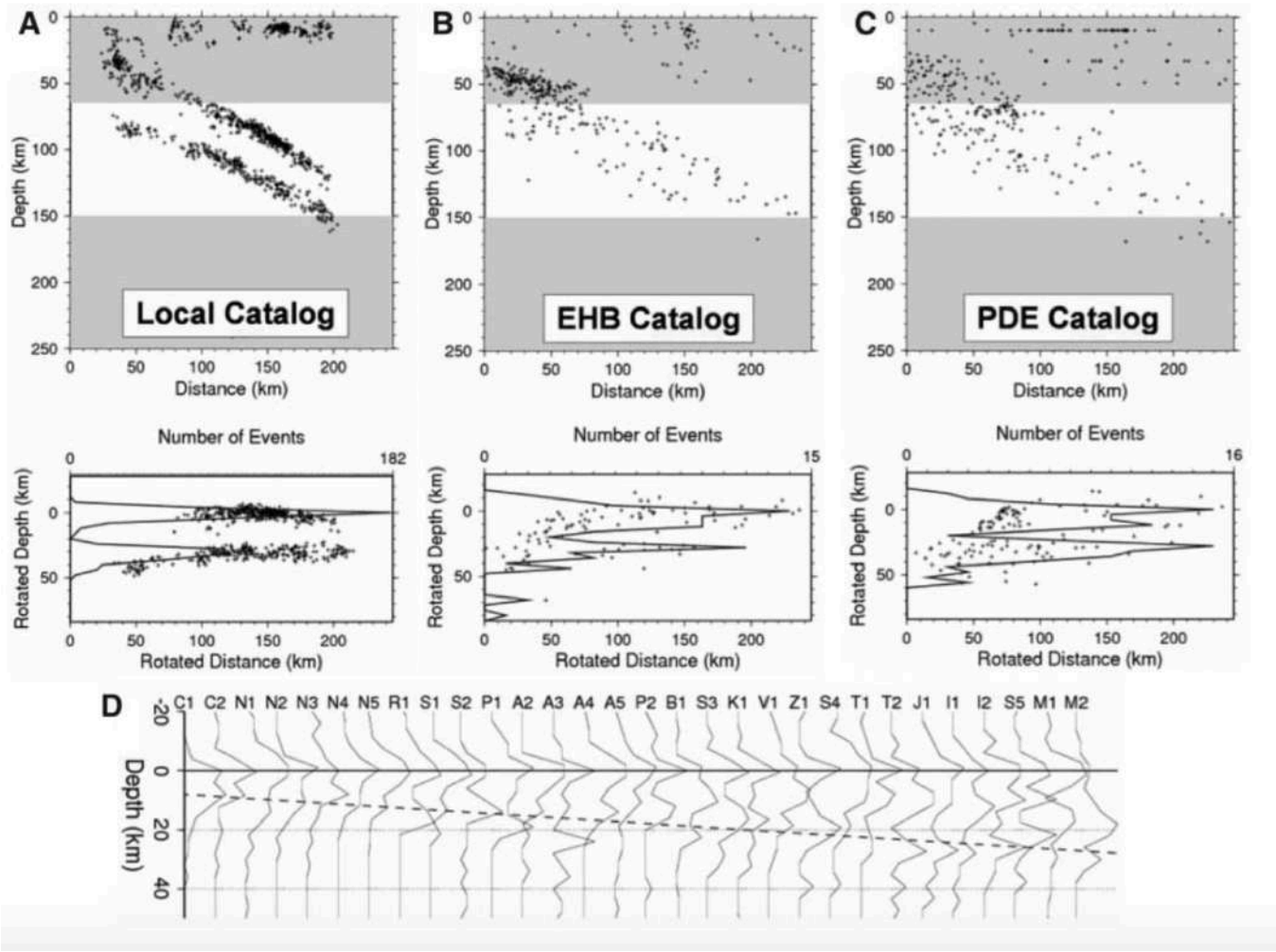

Brudzinsky et al. (2007)

Geodynamic models of outer rise faulting in the slab

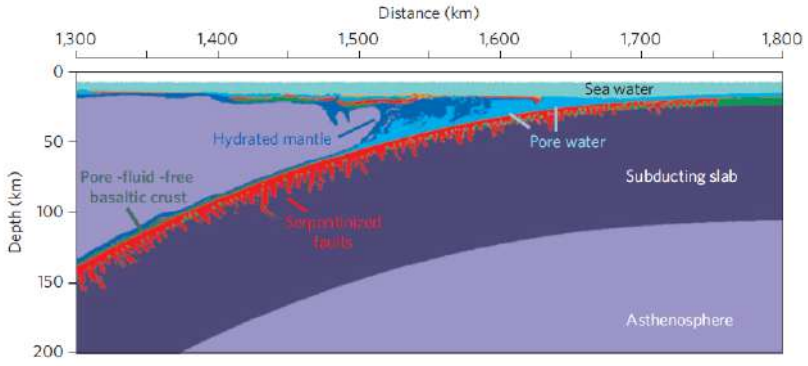

Faccenda et al. (2009)

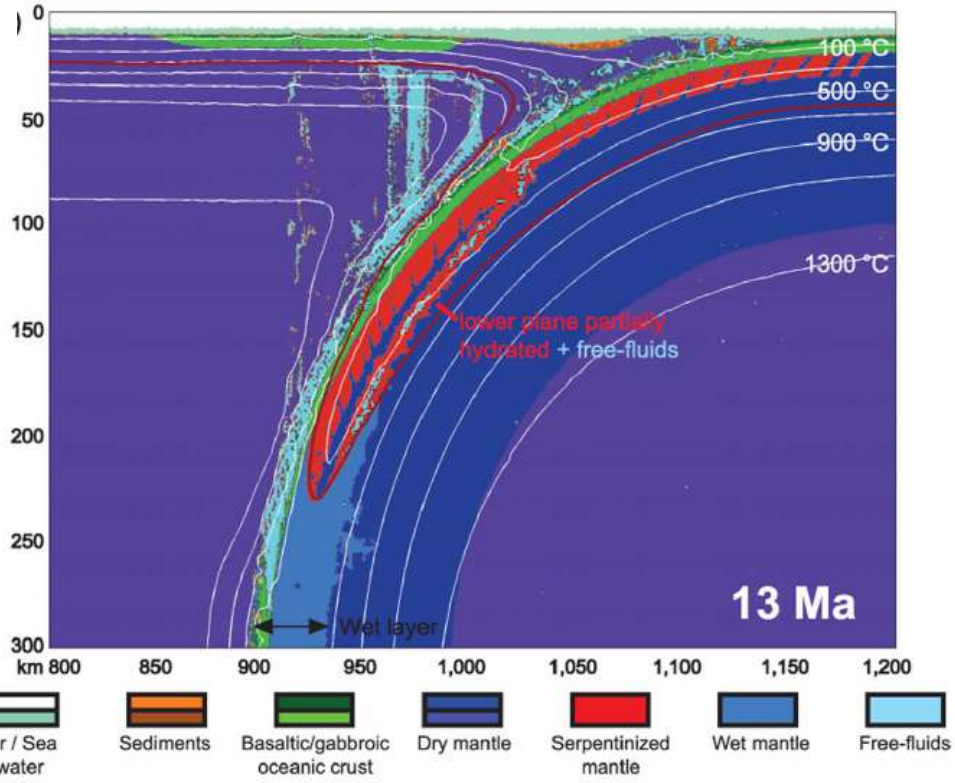

Faccenda et al. (2012)

Dehydration embrittlement

Figure 5.4-22: Model for intermediate-depth earthquakes.

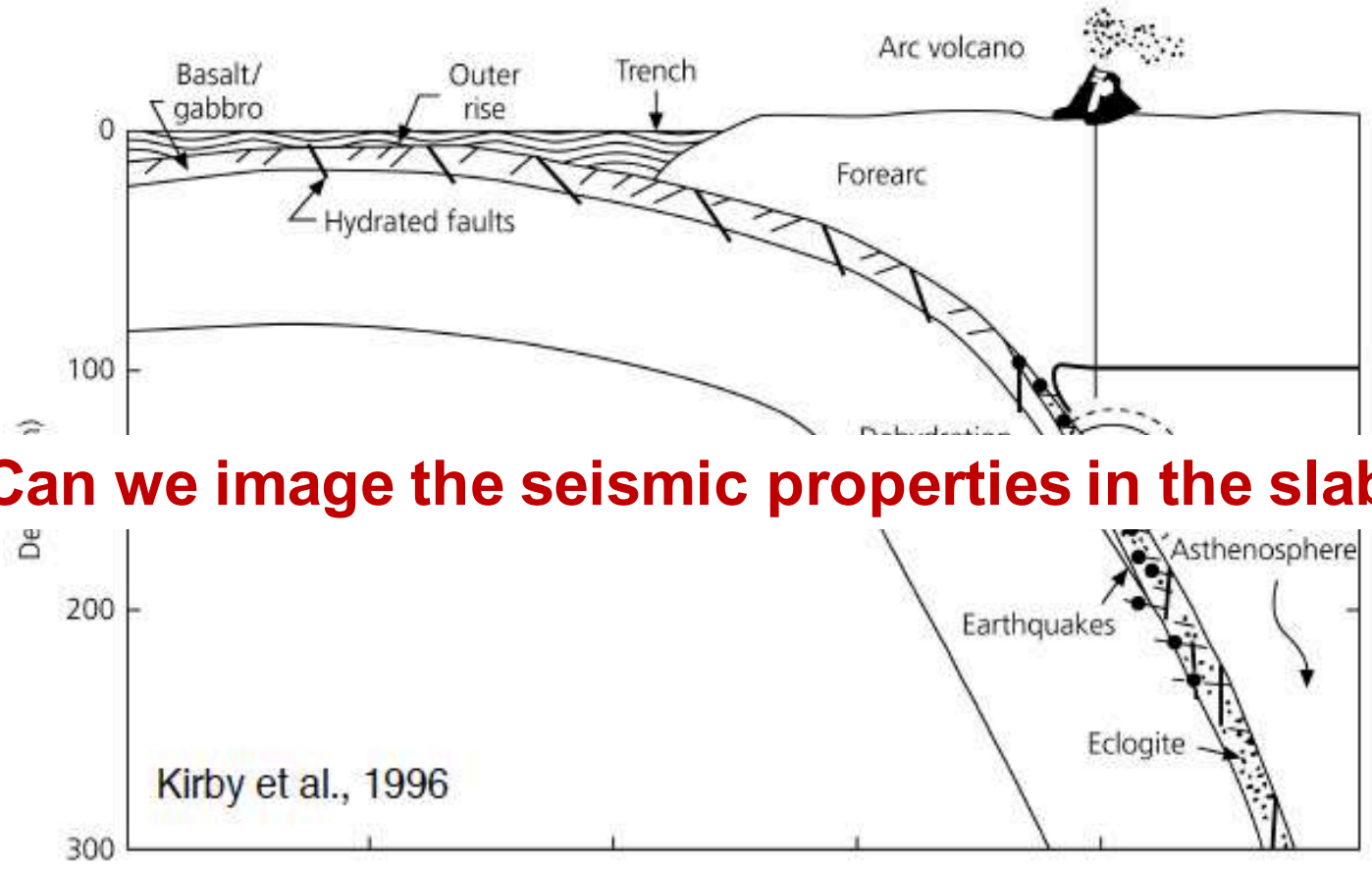

Can we image the seismic properties in the slab?

Tomography “The perfect example”: Japan

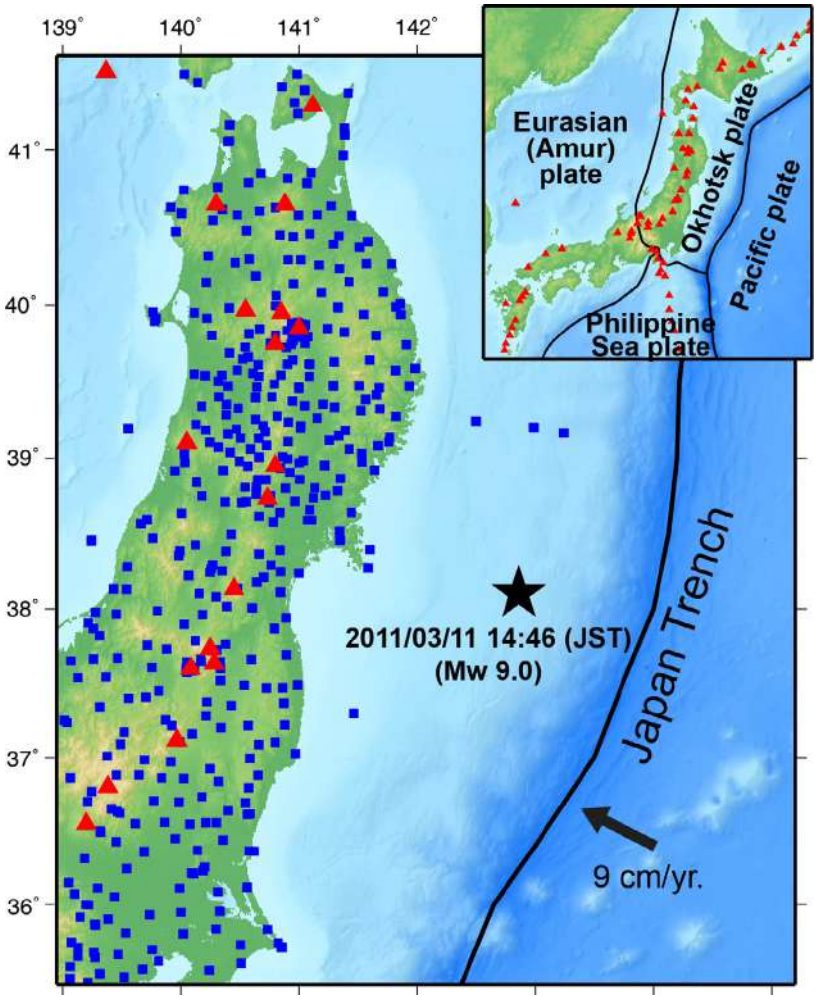

HighNet (e.g.: Huang&Zhao, 2013)

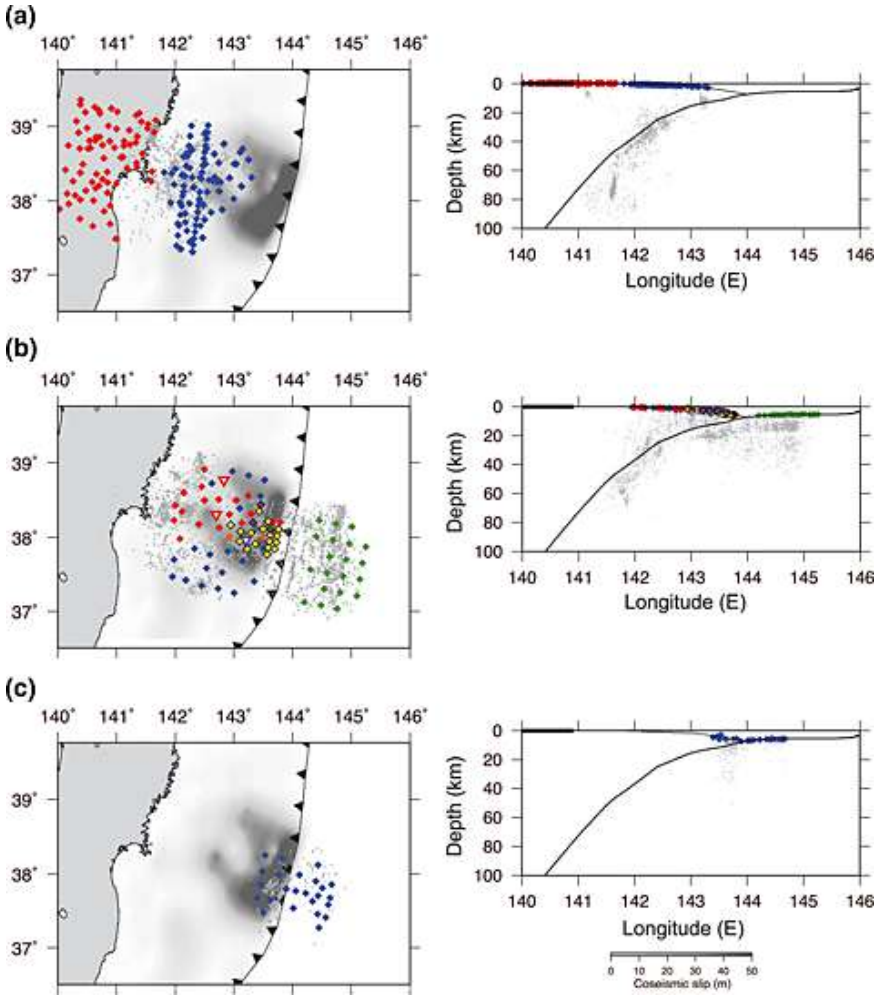

Temporary deployments (e.g. Yamamoto et al., 2014)

Physical properties along the interface

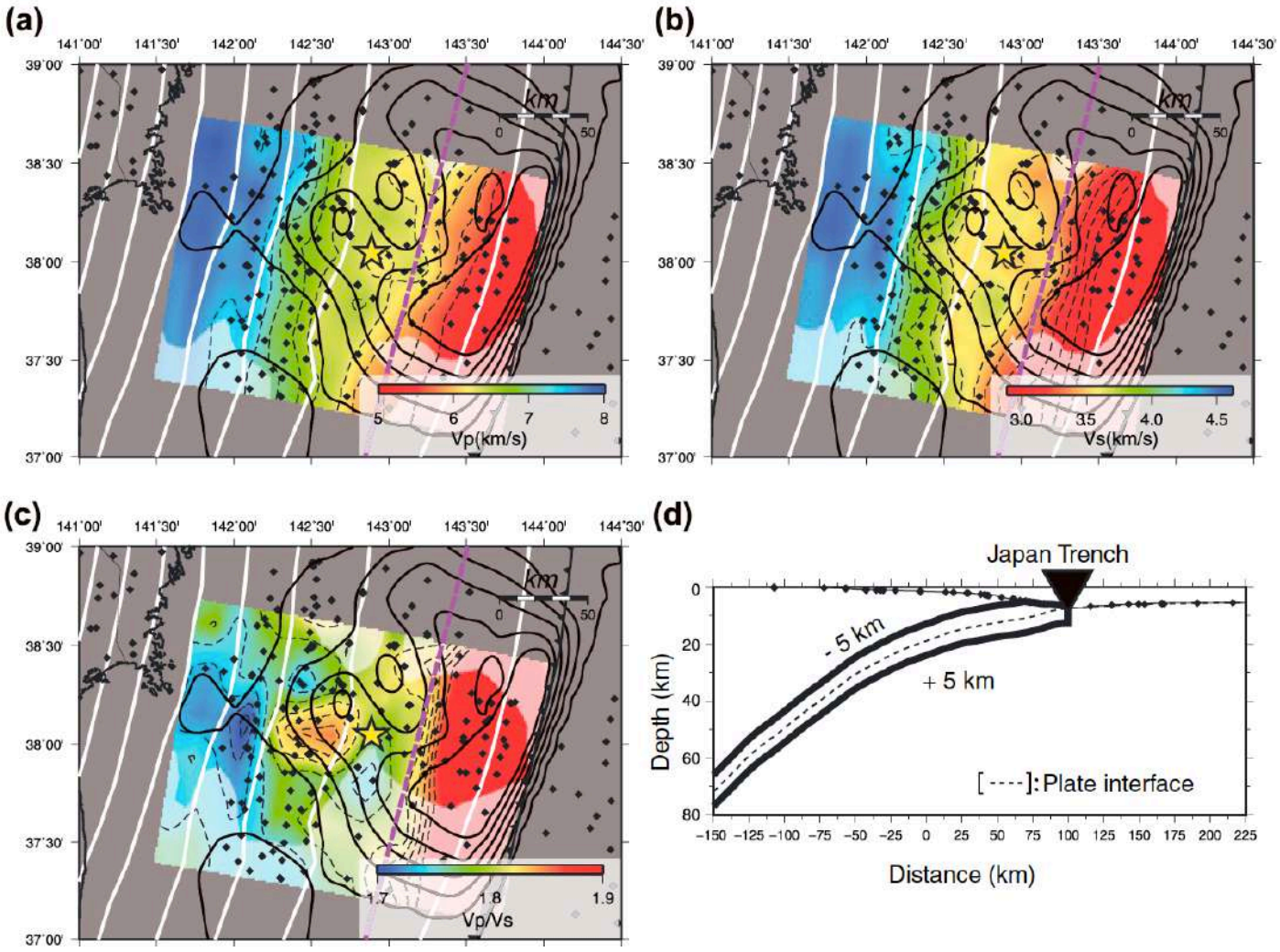

Yamamoto et al., 2014

Maule M_w 8.8 aftershock deployment (IMAD): pretty close to perfect

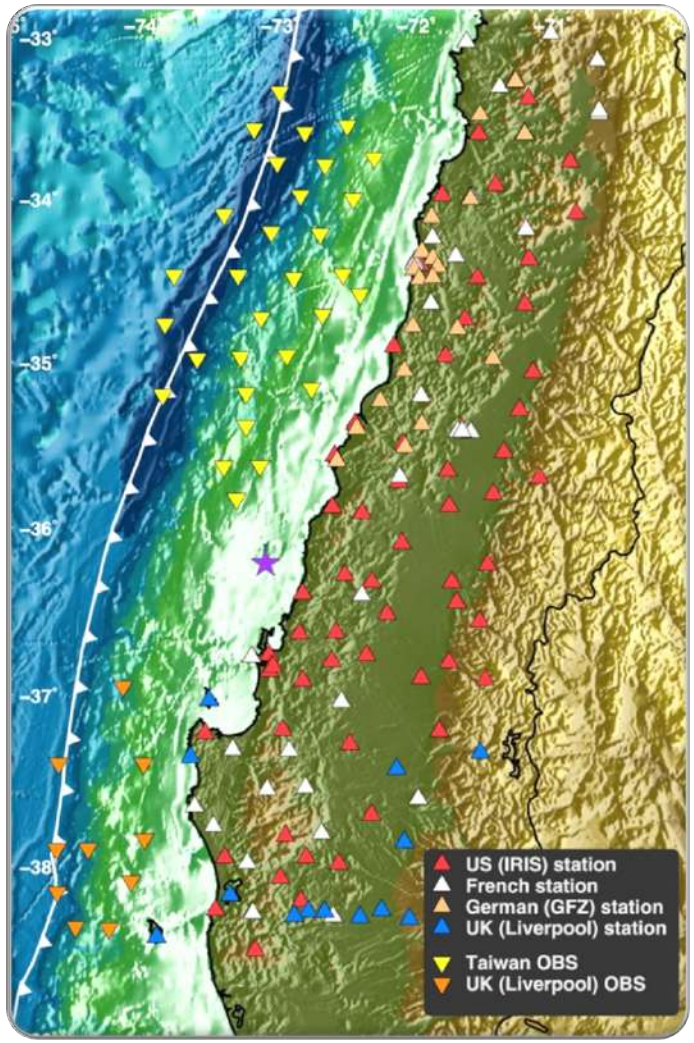

Unprecedented data set:

- International collaboration from the outset
- First stations in place in less than a week
- Open data policy from day one
- 200 stations (mainly broadband)
- 1TB of continuous high frequency data accessible through IRIS (or Liverpool)
- Onshore and offshore deployment covering the length of the rupture areas
- Travel time tomography data set:
  - 670 selected events for optimizing spatial and depth resolution
  - 38,000 P wave onset times
  - 14,000 S wave onset times

Rietbrock et al., 2013; Beck et al., 2014

Traveltime tomography results (2D)

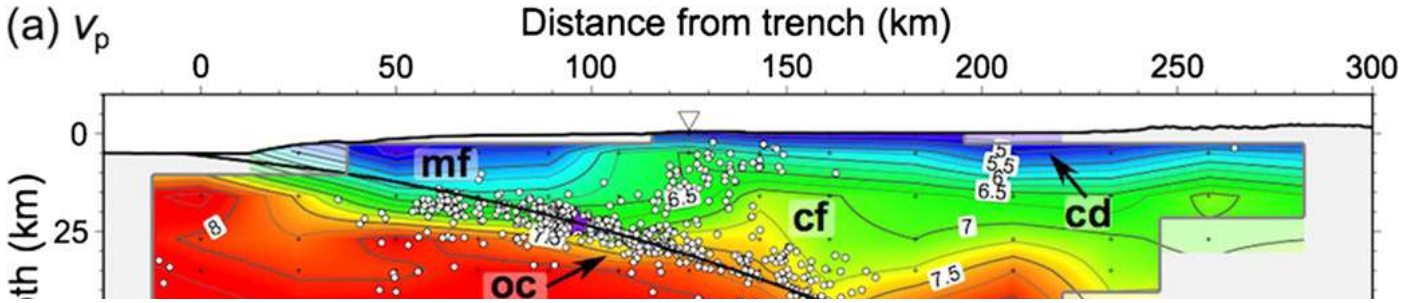

Current experiments and technology (based on traveltimes): Structures in the Oceanic crust are hard to resolve (even at megathrust depth)

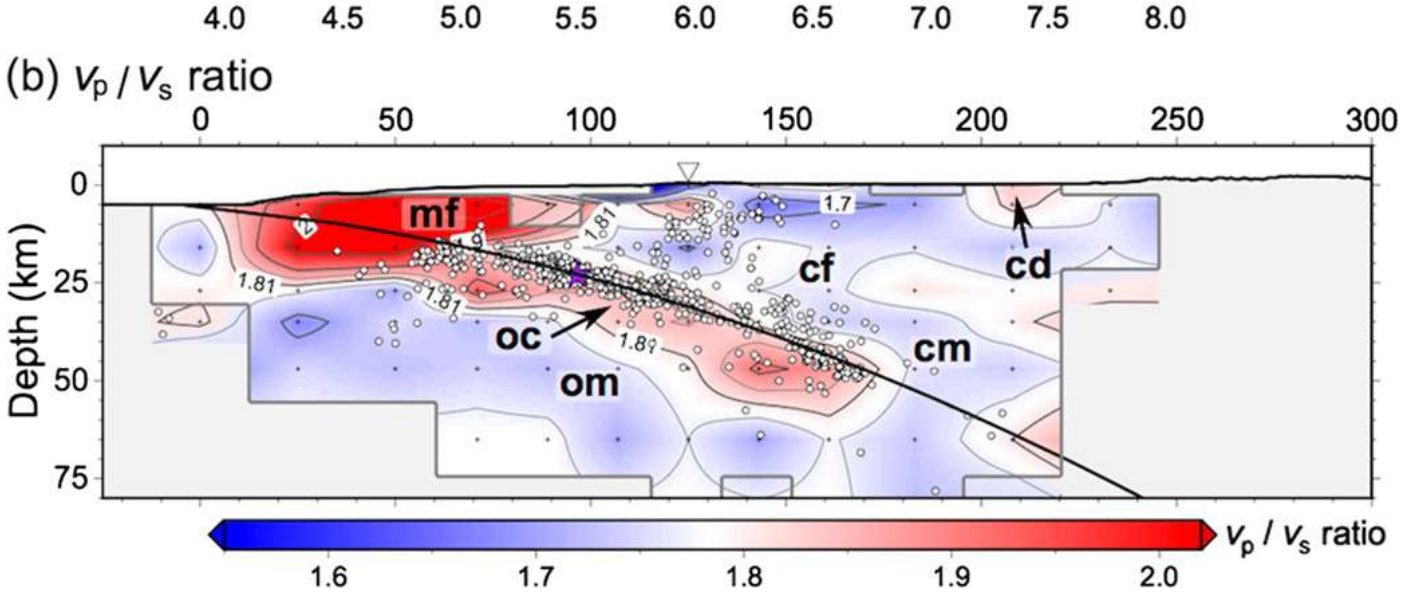

Hicks et al., 2014

Slab surface⇔ earthquake locations

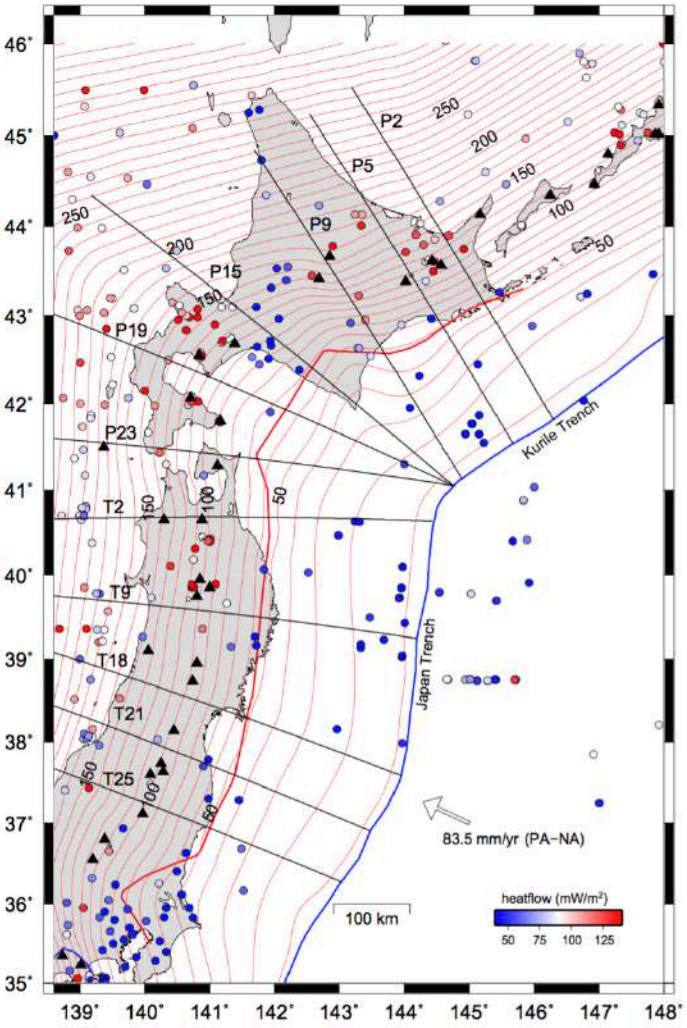

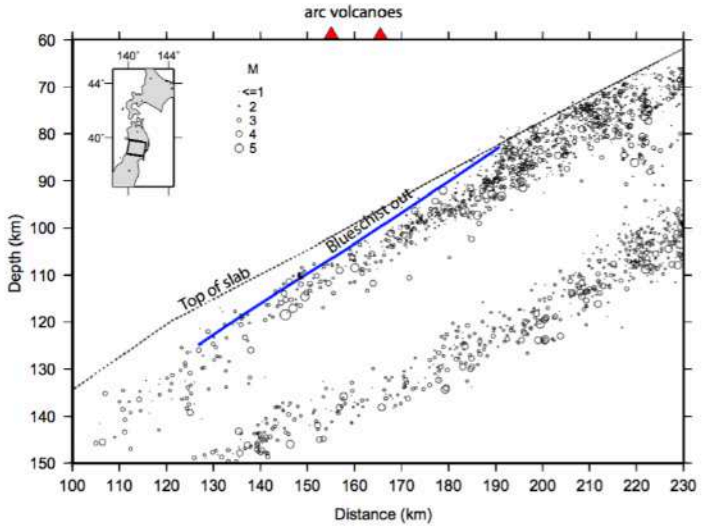

Fig. 2. Seismicity in the Pacific slab below Tohoku. Modified after Kita et al. (2006) and Abers et al. (2012). The earthquakes from 120 km wide box shown in the insert are projected on the center cross section, normal to the trench. This region is approximately bordered by profiles T9 and T18 in Fig. 1. The upper plane of seismicity is within 10 km (in depth) from the top of the slab and tends to be deeper in the slab as the slab descends. The blueschist-out boundary (predicted for this profile following the methods by van Keken et al., 2011) seems to delimit the deepest seismicity in the upper plane.

cant H_2O (~2–3 wt %). The crust is generally assumed to be dry after the lawsonite-out reaction, which does not happen until significantly higher temperature (~650 °C at 3 GPa,

vanKecken al. (2012)

Thermal modelling ⇔ Petrological interpretation

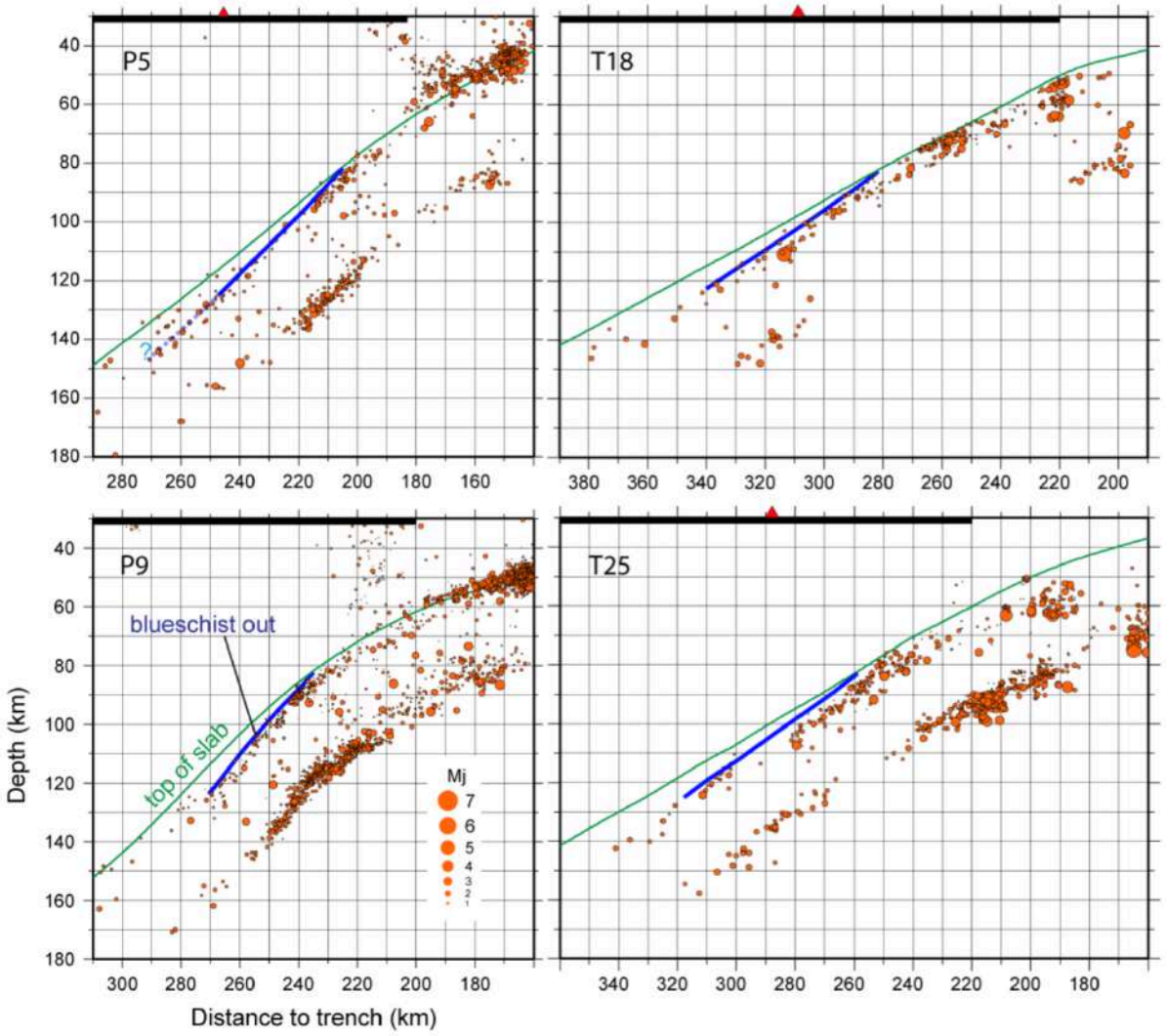

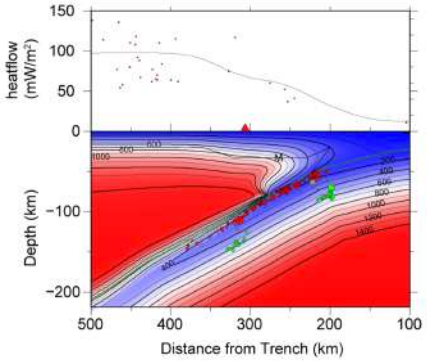

vanKecken al. (2012)

Dehydration embrittlement

Figure 5.4-22: Model for intermediate-depth earthquakes.

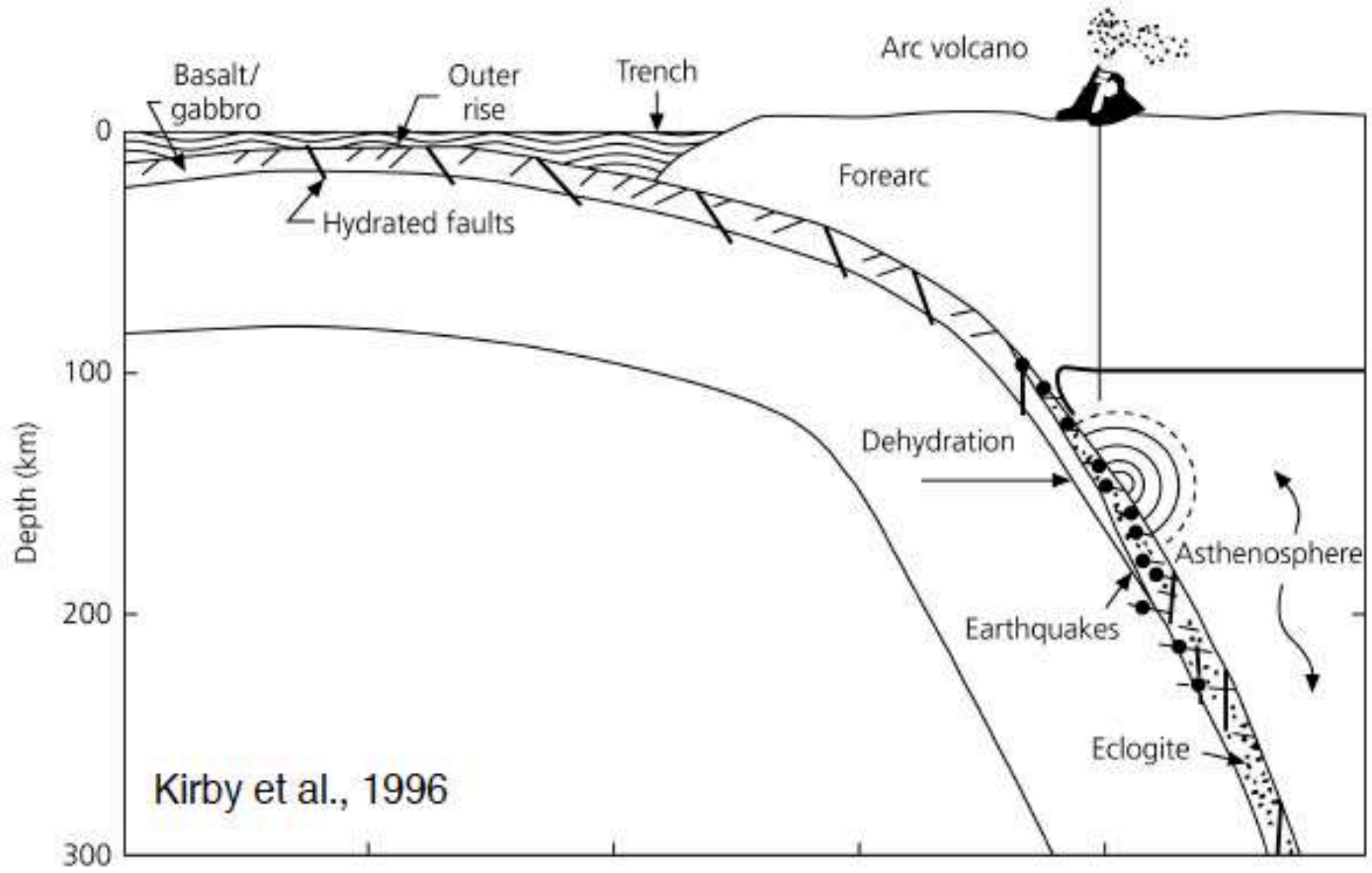

The idea of guided waves

ELSEVIER

Earth and Planetary Science Letters 176 (2000) 323–330

EPSL

www.elsevier.com/locate/epsl

Hydrated subducted crust at 100–250 km depth

Geoffrey A. Abers *

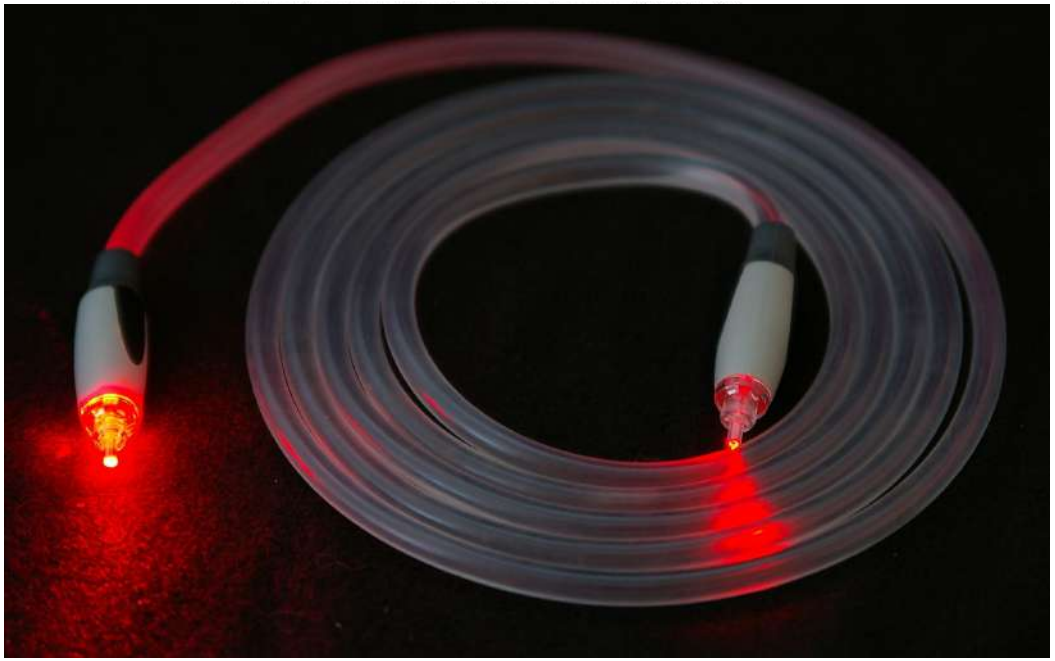

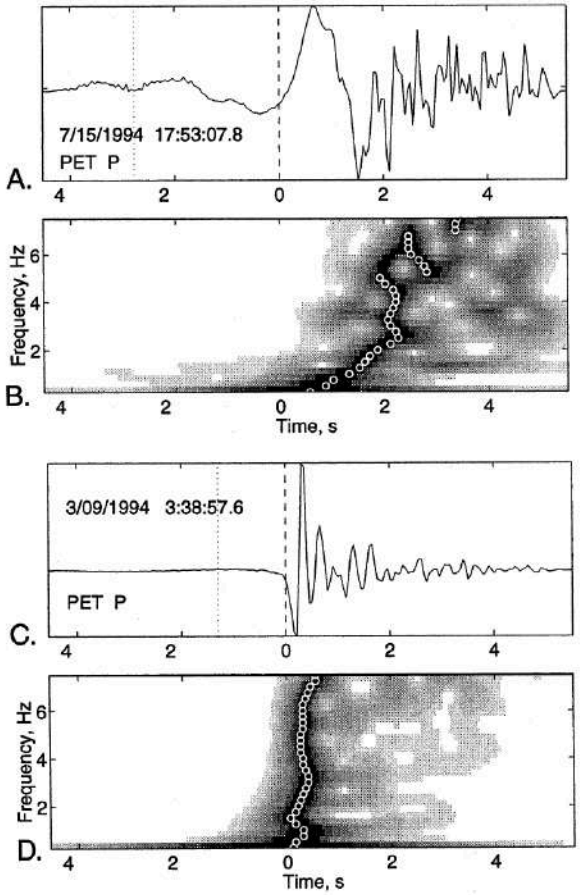

Abers 2000

Peculiar P-wave arrivals in subduction zones

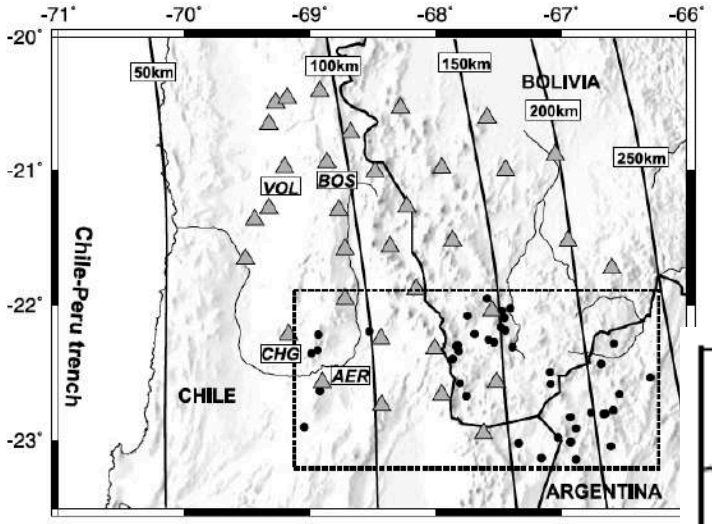

Figure 1. Map of the ANCORP'96 temporary seismic network consisting of 32 short-peric (triangles) equipped with Mark L-4A-3D sensors. Solid lines represent depth contours. The d contains events (dots) recorded at station AER forming an updip section centered at 22.58°S. T were located by *Rietbrock et al.* [1997] using a local earthquake tomographic method.

AER

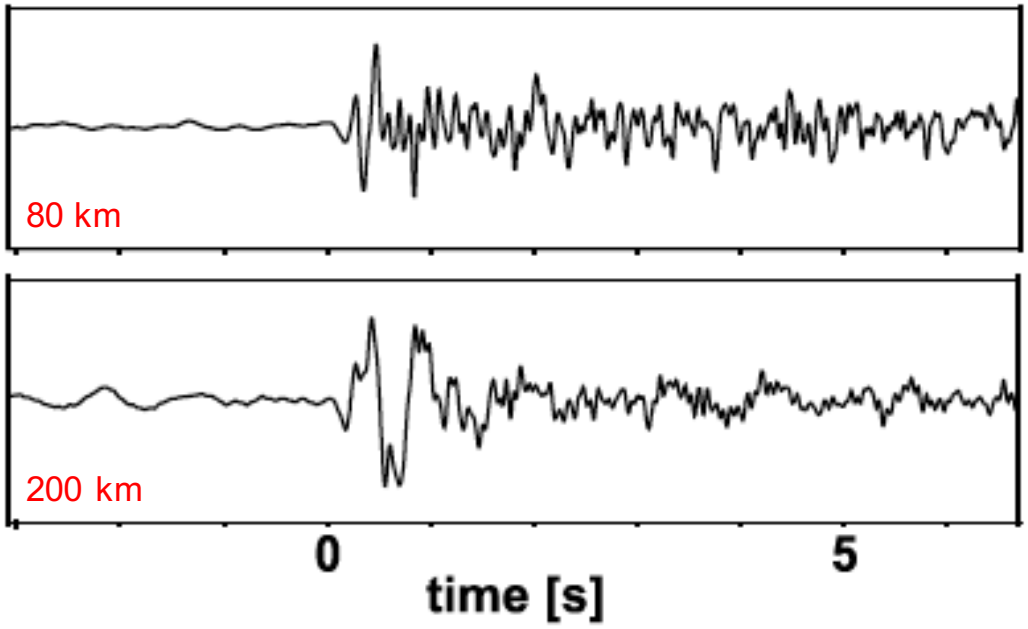

Guided waves are sensitive to slab structure, but why do we observe them?

Martin et al. (2003, 2005, 2006)

Peculiar P-wave arrivals

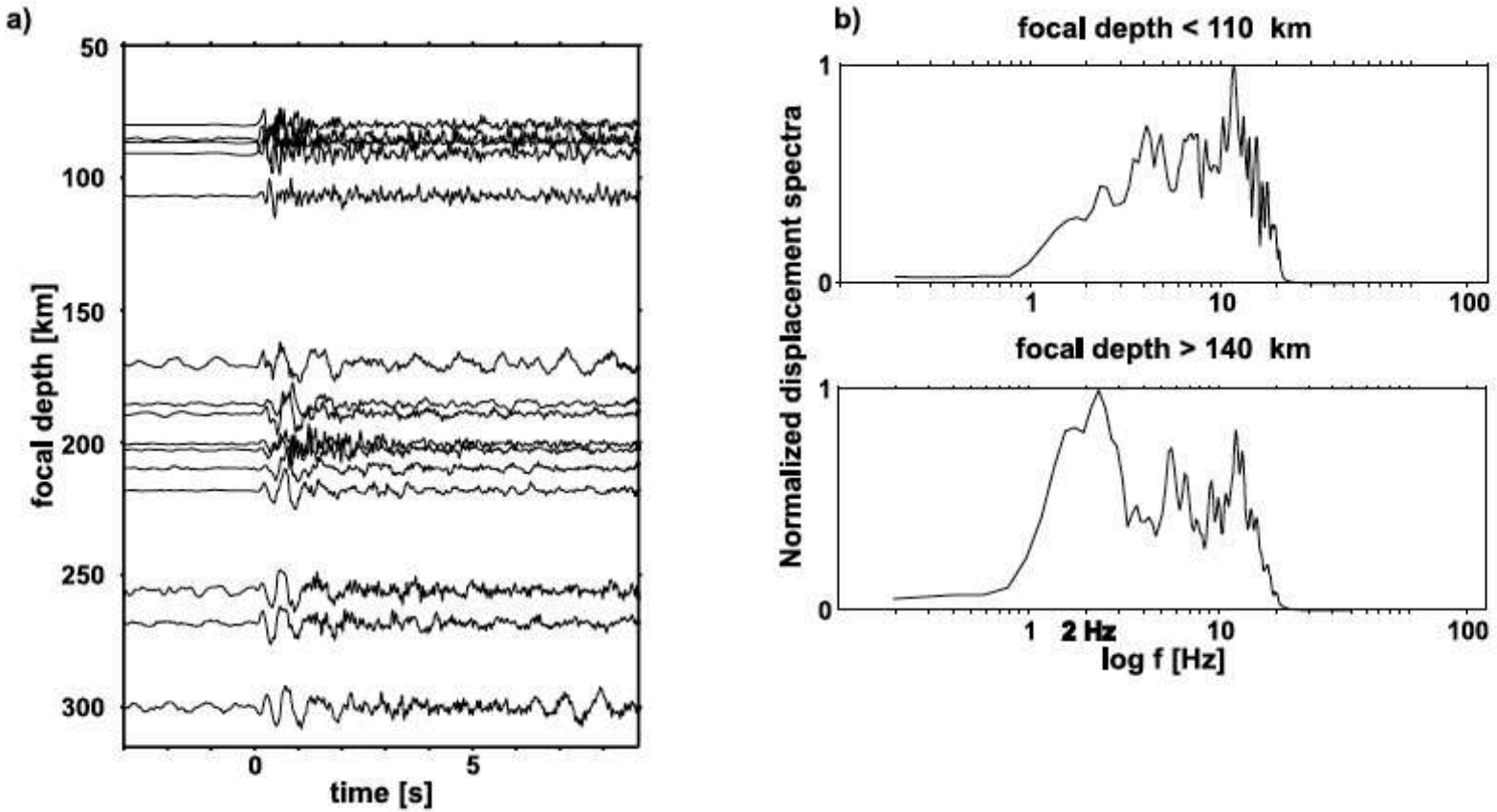

Figure 3. (a) Aligned *P* onsets of selected events recorded at station AER plotted by focal depth (for further explanations see Figure 2). (b) Stacked displacement spectra of onsets (first 2 s) of all events contained in the updip section (see Figure 1) with focal depth <110 km and >140 km, respectively.

Martin et al. (2003, 2005, 2006)

‘Simple’ model 1

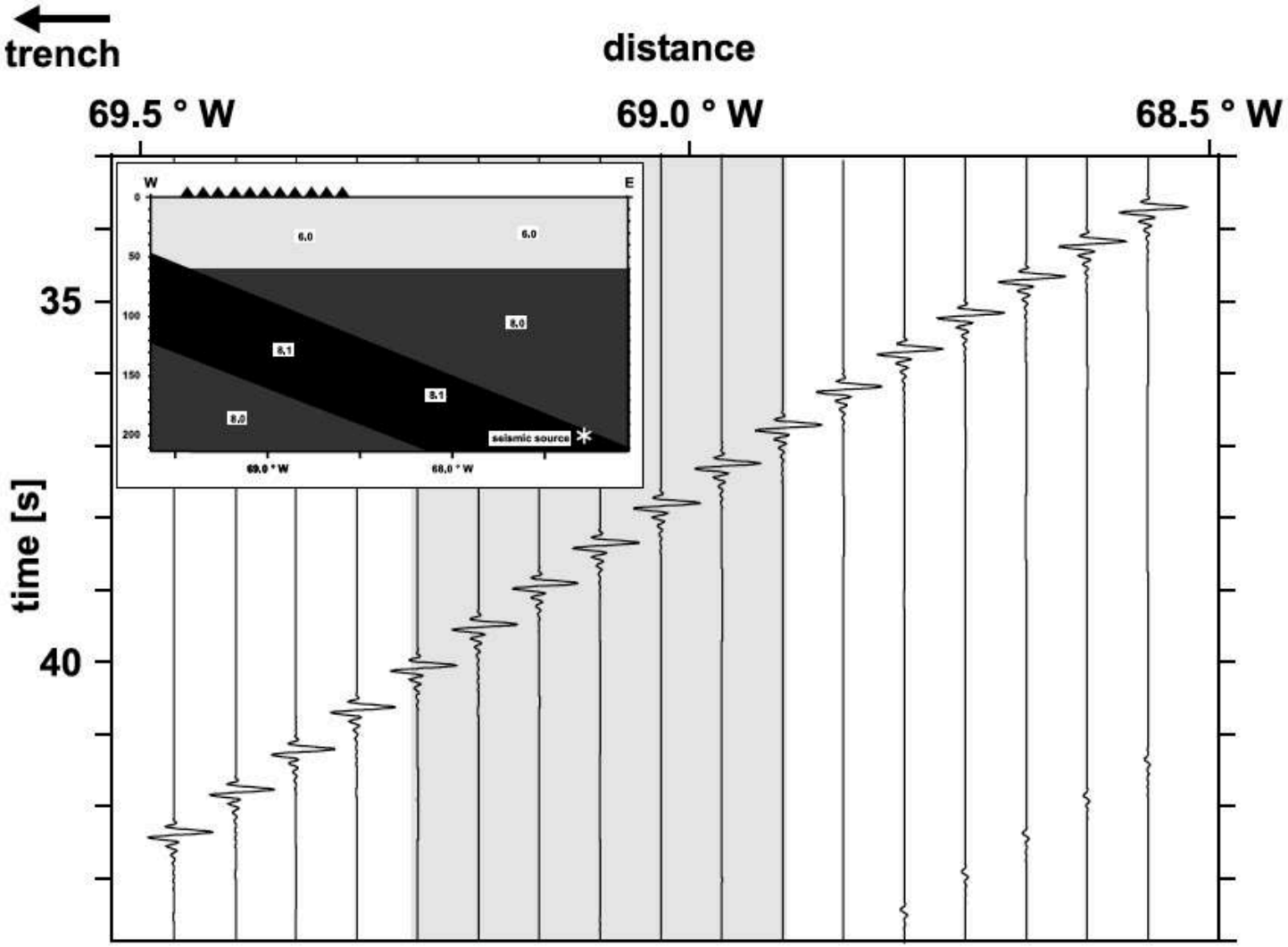

Martin et al. (2003)

‘Simple’ model 2

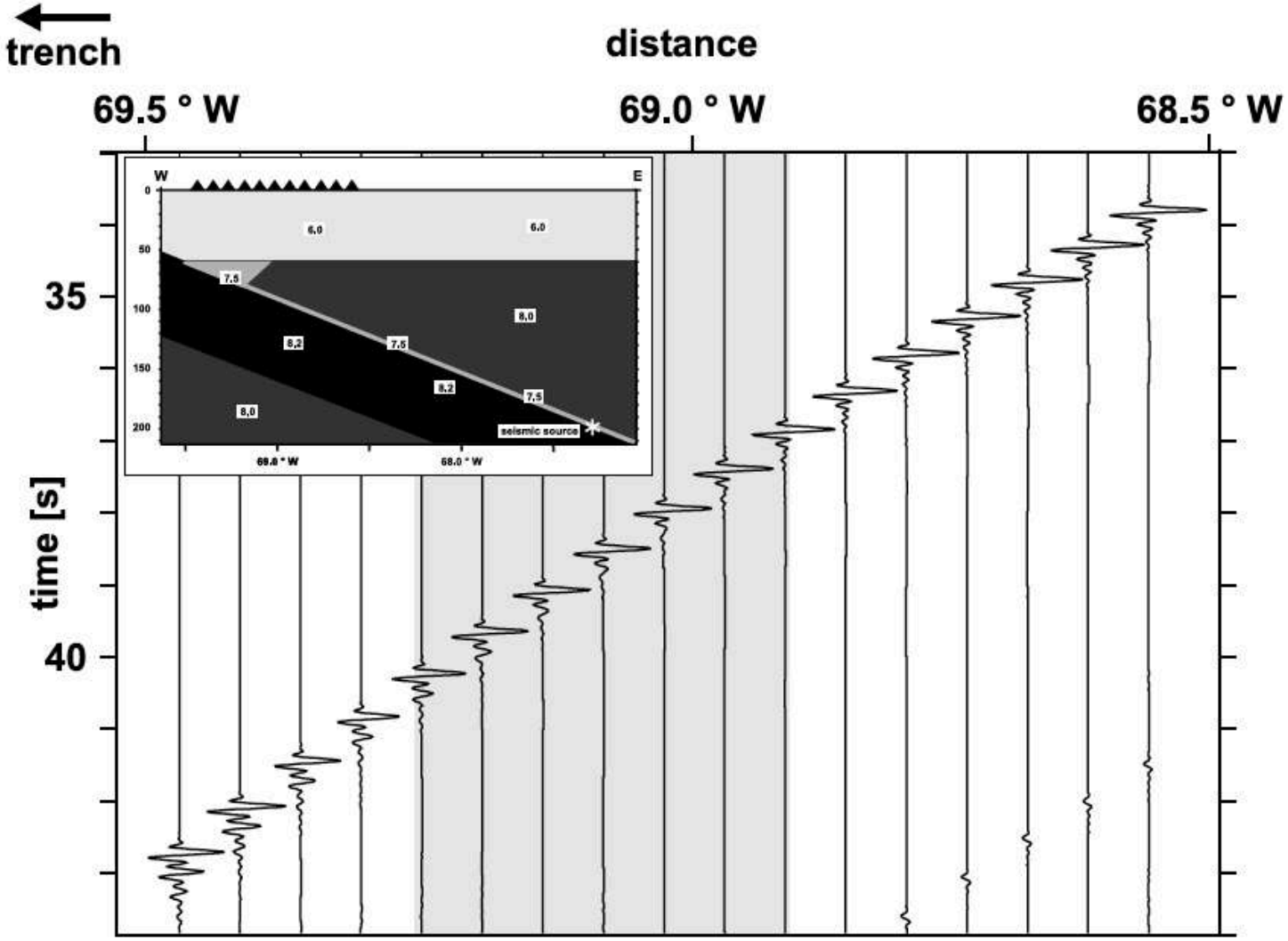

Martin et al. (2003)

Bending lithospheric slab: mechanism to decouple seismic energy

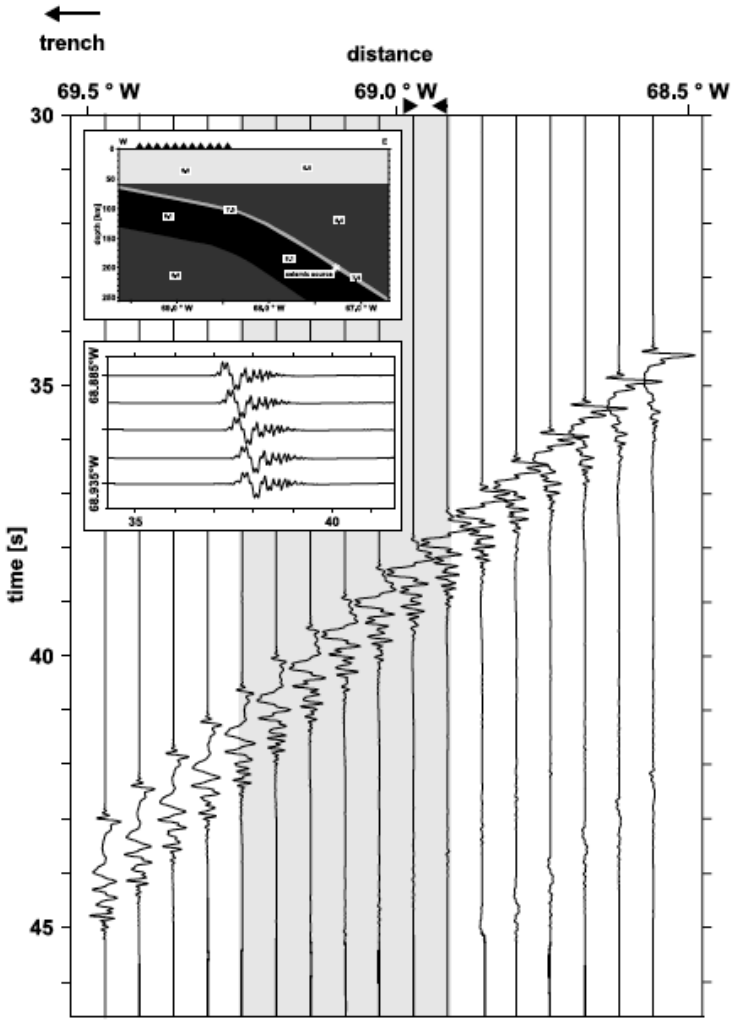

Martin et al. (2003)

Geometry given by intermediate depth seismicity:

Wadati-Benioff-Zone

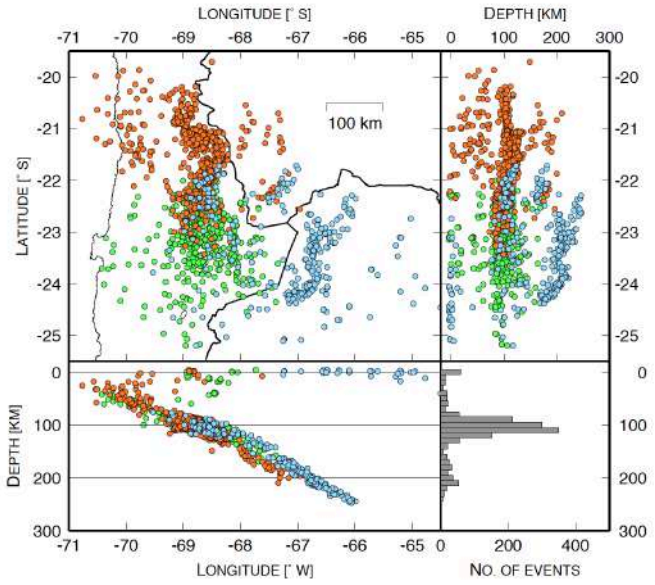

Schurr (2000)

Snapshots of wavefield

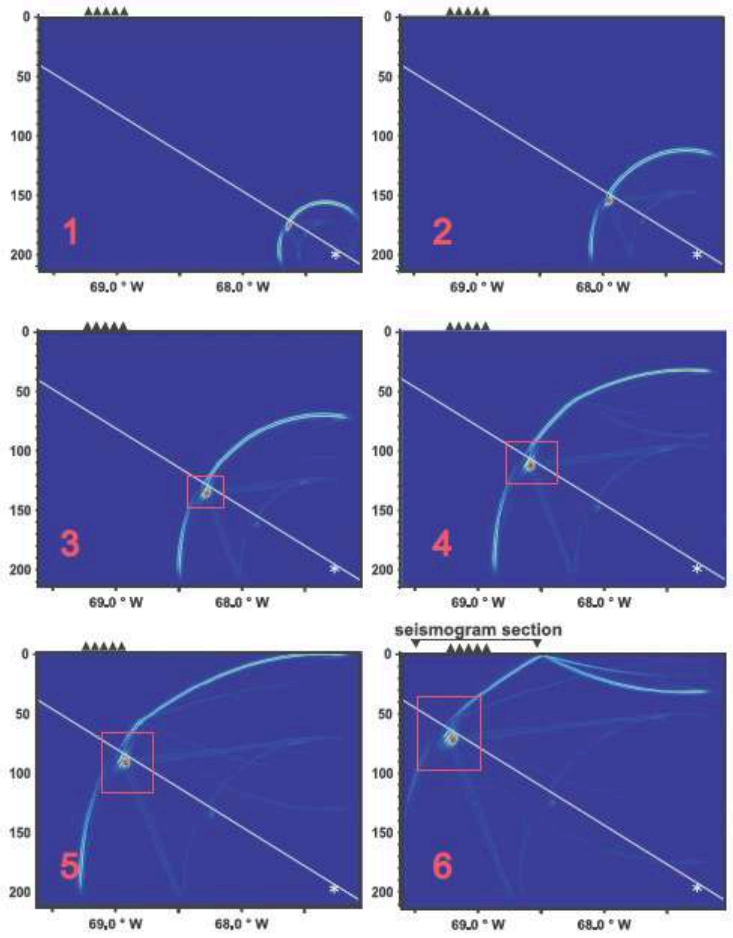

straight

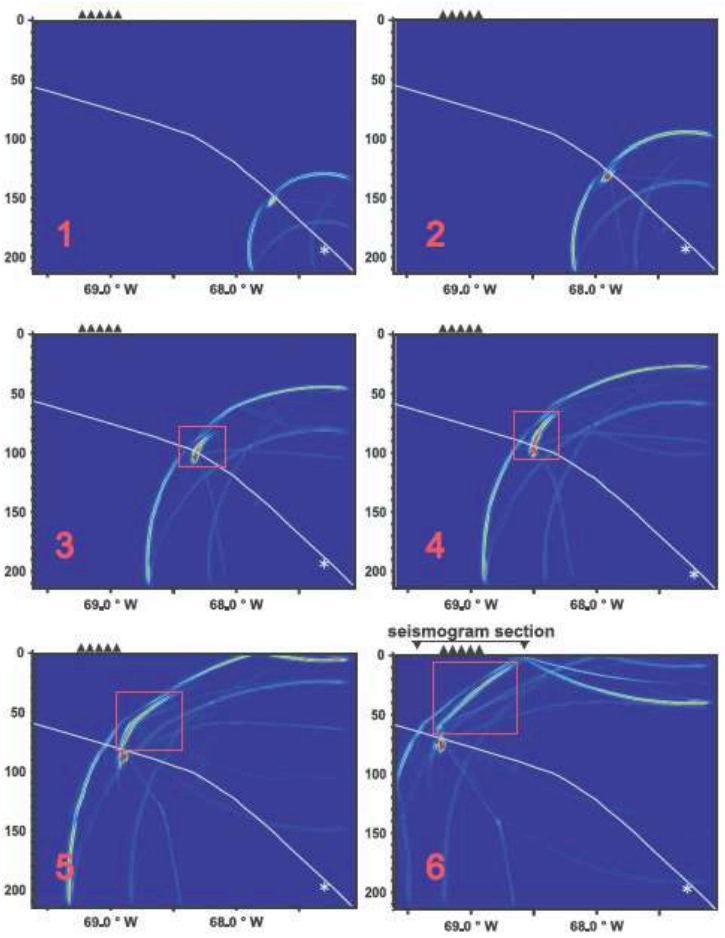

bended

Earthquake location matters

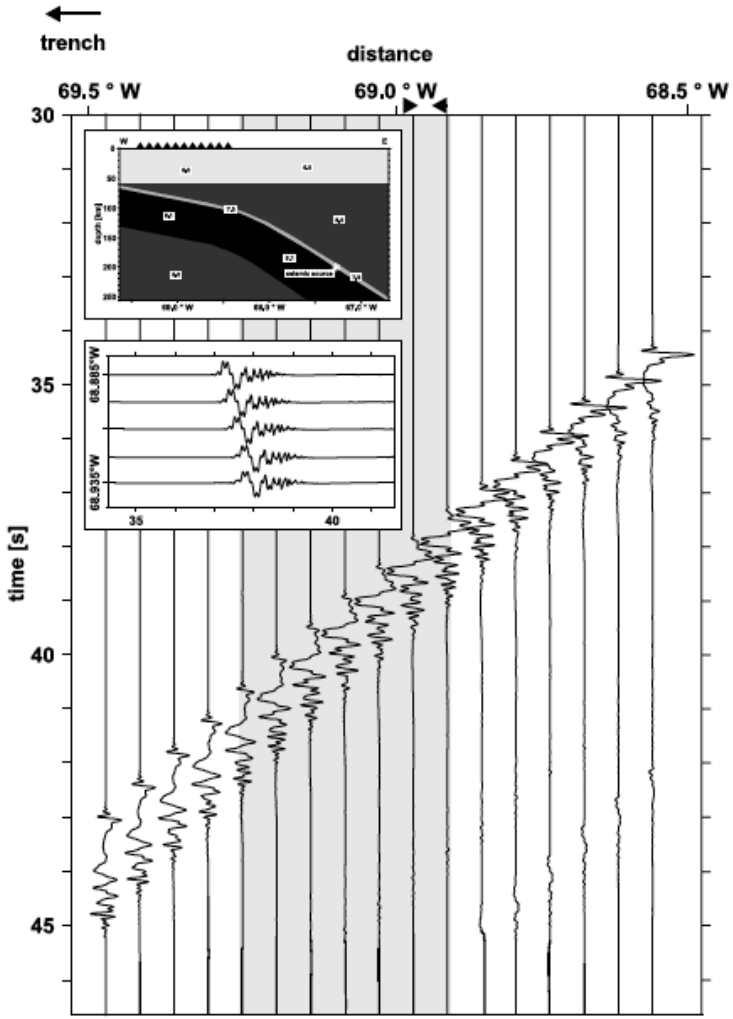

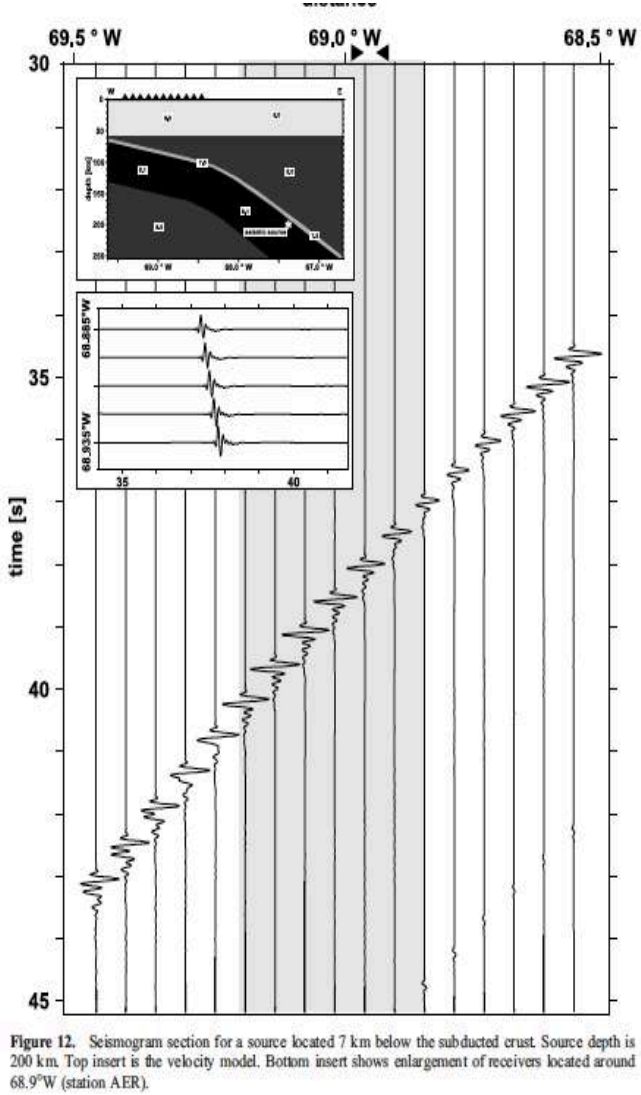

Figure 12. Seismogram section for a source located 7 km below the subducted crust. Source depth is 200 km. Top insert is the velocity model. Bottom insert shows enlargement of receivers located around 68.9°W (station AER).

Martin and Rietbrock (2006)

Source radiation matters

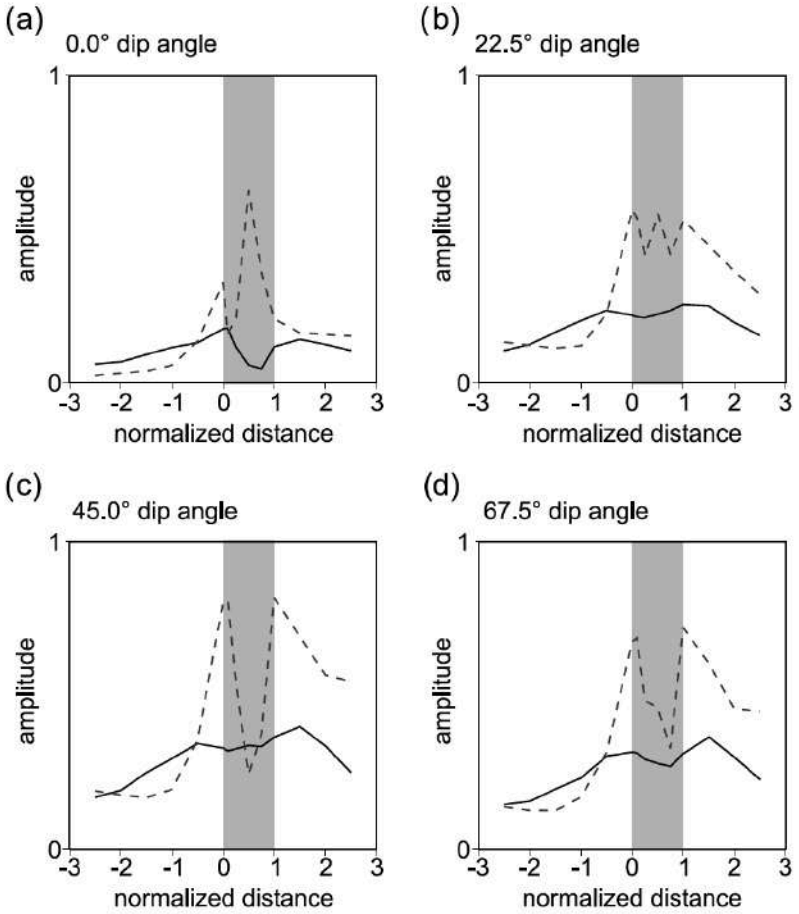

Down dip extension

High frequency energy

Low frequency energy

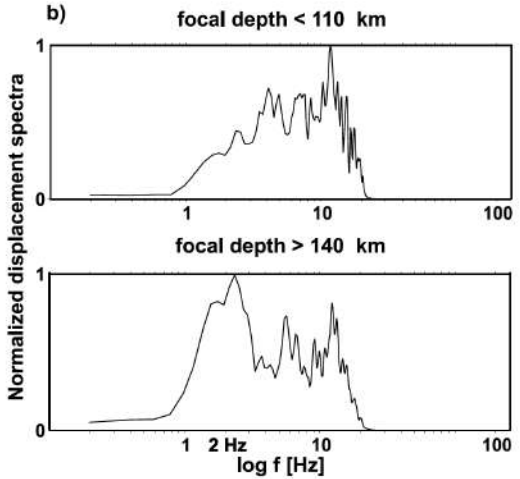

Martin and Rietbrock (2006)

Bending lithospheric slab: low velocity lower crust

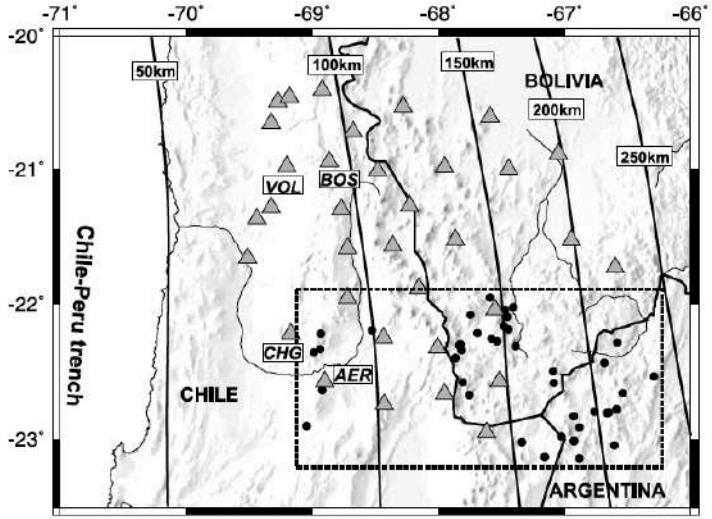

Figure 1. Map of the ANCORP'96 temporary seismic network consisting of 32 short-period stations (triangles) equipped with Mark L-4A-3D sensors. Solid lines represent depth contours. The dashed line contains events (dots) recorded at station AER forming an updip section centered at 22.58°S. The events were located by *Rietbrock et al.* [1997] using a local earthquake tomographic method.

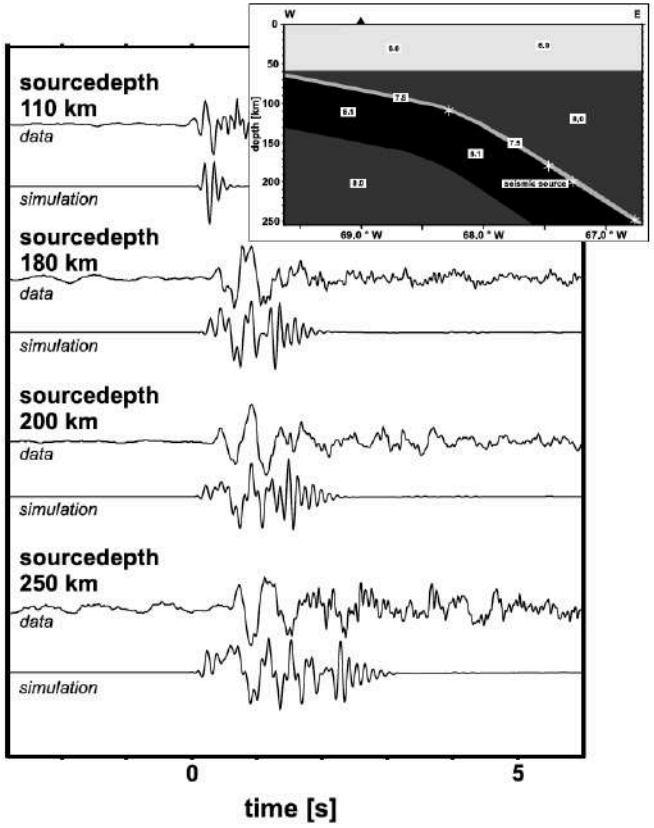

Figure 10. Synthetics (receiver at 69°W) for sources located inside the low-velocity layer (at 0.3 km perpendicular distance to subducted oceanic Moho) at various depths and ANCORP data (recorded at station AER) for the corresponding depths. Signals are aligned using a cross-correlation algorithm. Insert shows the velocity model and source positions.

1. **<4.5km thick low velocity layer down to 160-180 km**
2. **Velocity reduction of ~ 7%**
3. **Eqs are located inside or just below the low velocity layer**

Martin et al. (2003, 2005, 2006)

Guided waves: A high Resolution Tool to Test Slab Structure

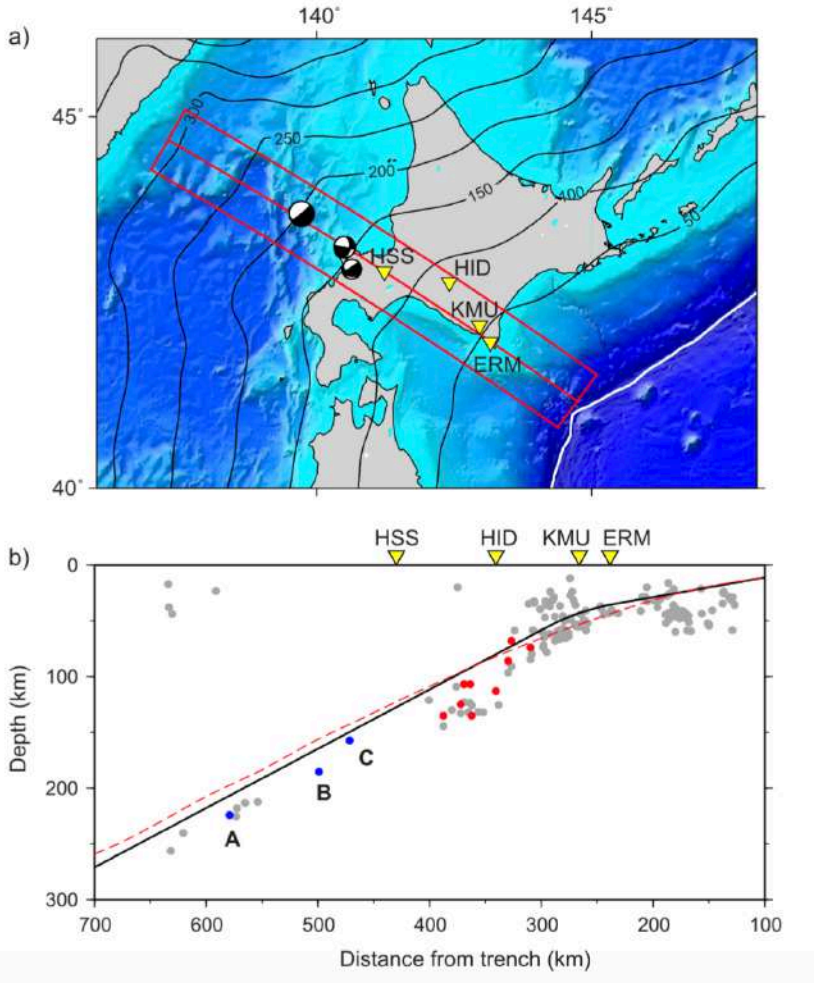

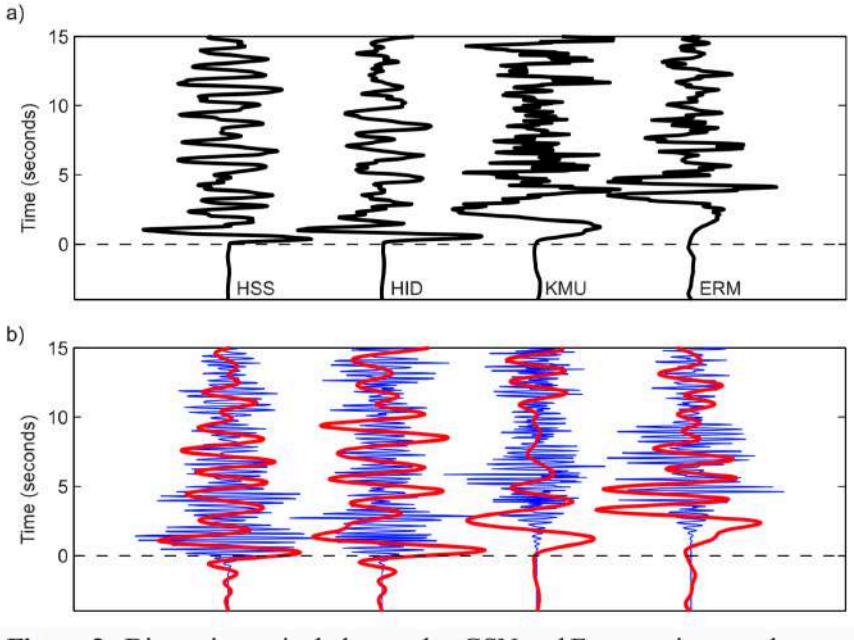

Clear dispersion observed

Japanese subduction zone

Garth&Rietbrock (2014a,b)

Propagating wavefield:
Long interaction with the slab!

Thickness of low velocity layer: 8km
Velocities: 7.2 to 7.5 km/s clear dependence with depth

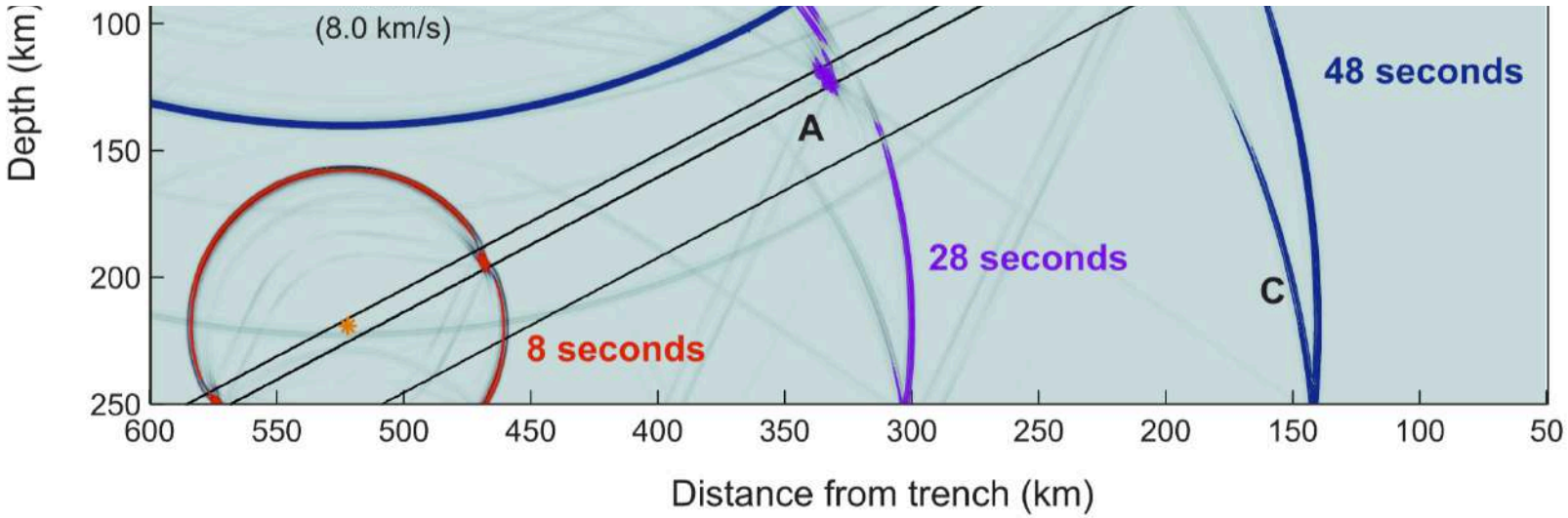

Garth&Rietbrock (2014b)

Guided waves: A high Resolution Tool to Test Slab Structure

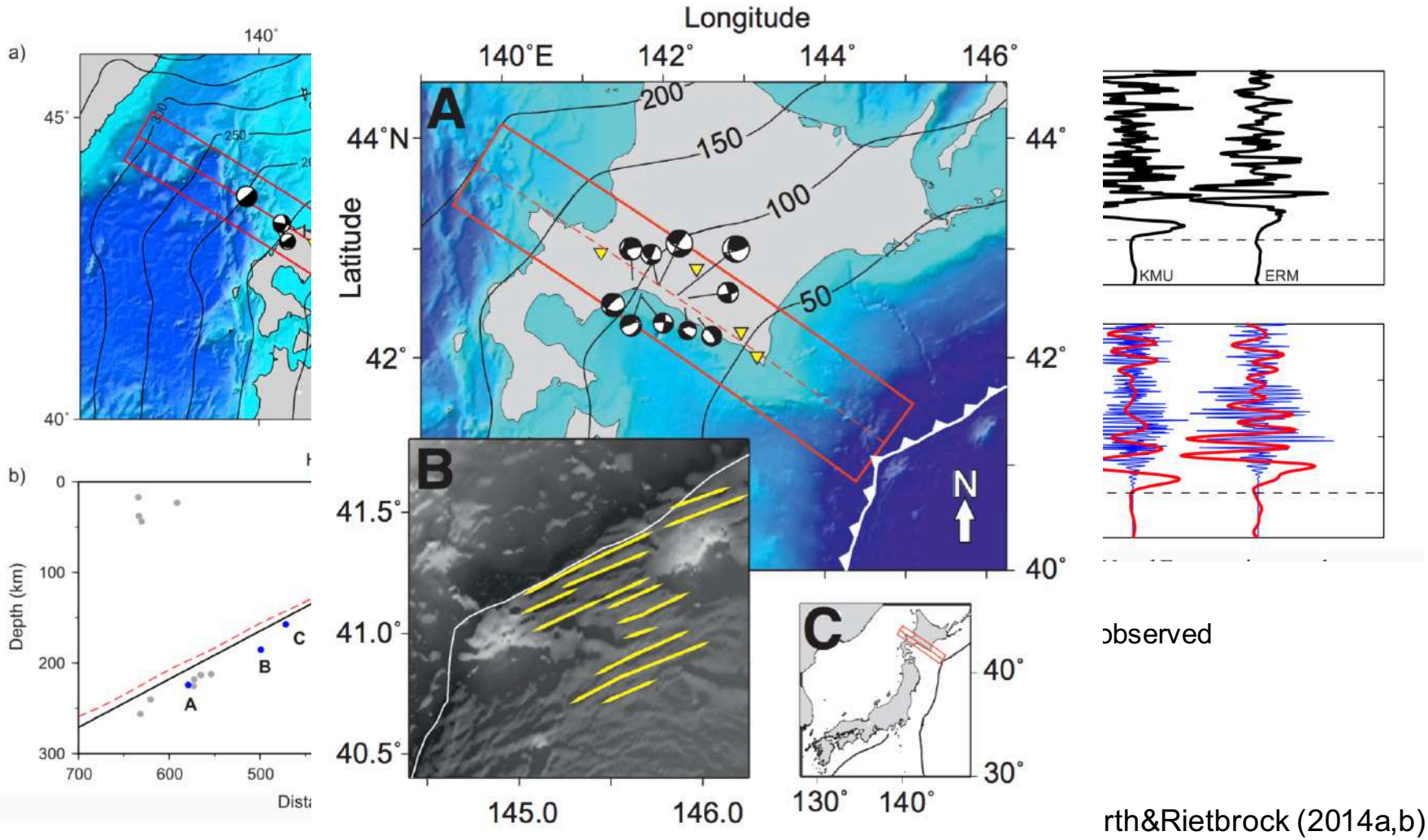

observed

rth&Rietbrock (2014a,b)

Hydrated faults have to exist

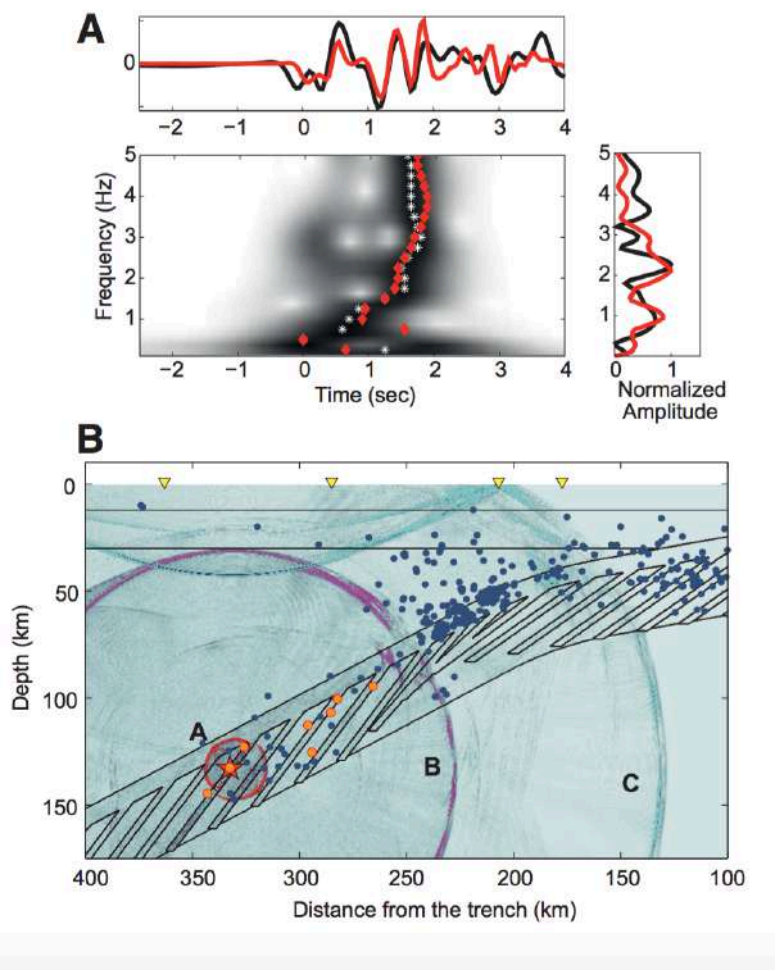

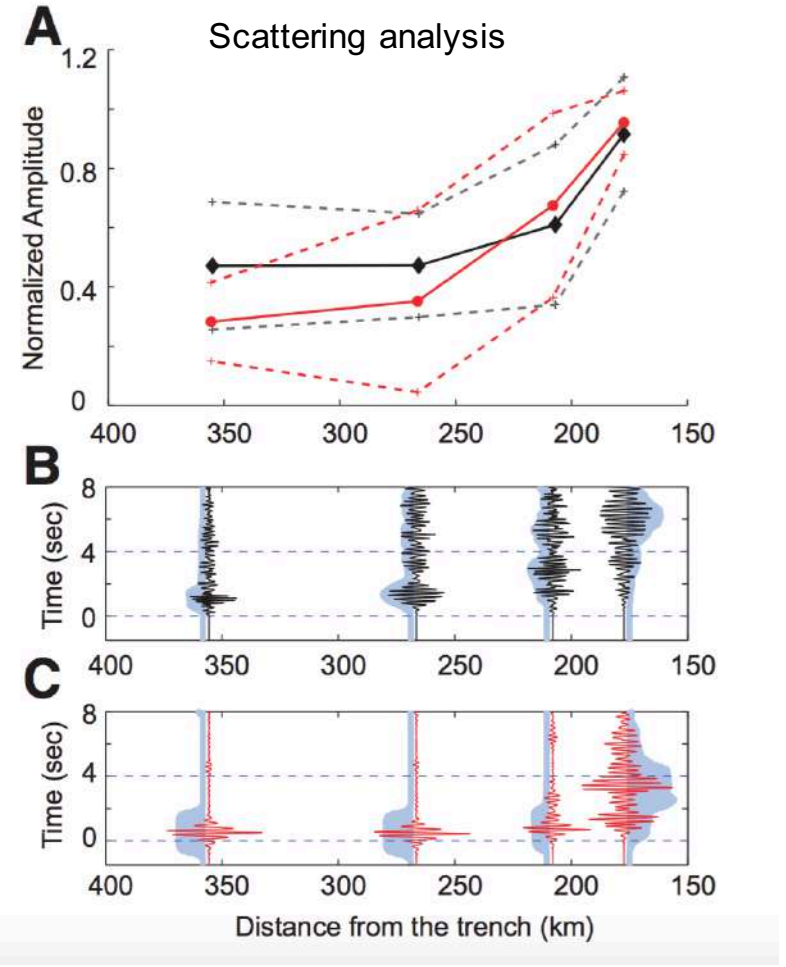

Garth&Rietbrock (2014a)

1) LVZ on top of the slab (~200km & 8km width)
2) LV faults deeply penetrating

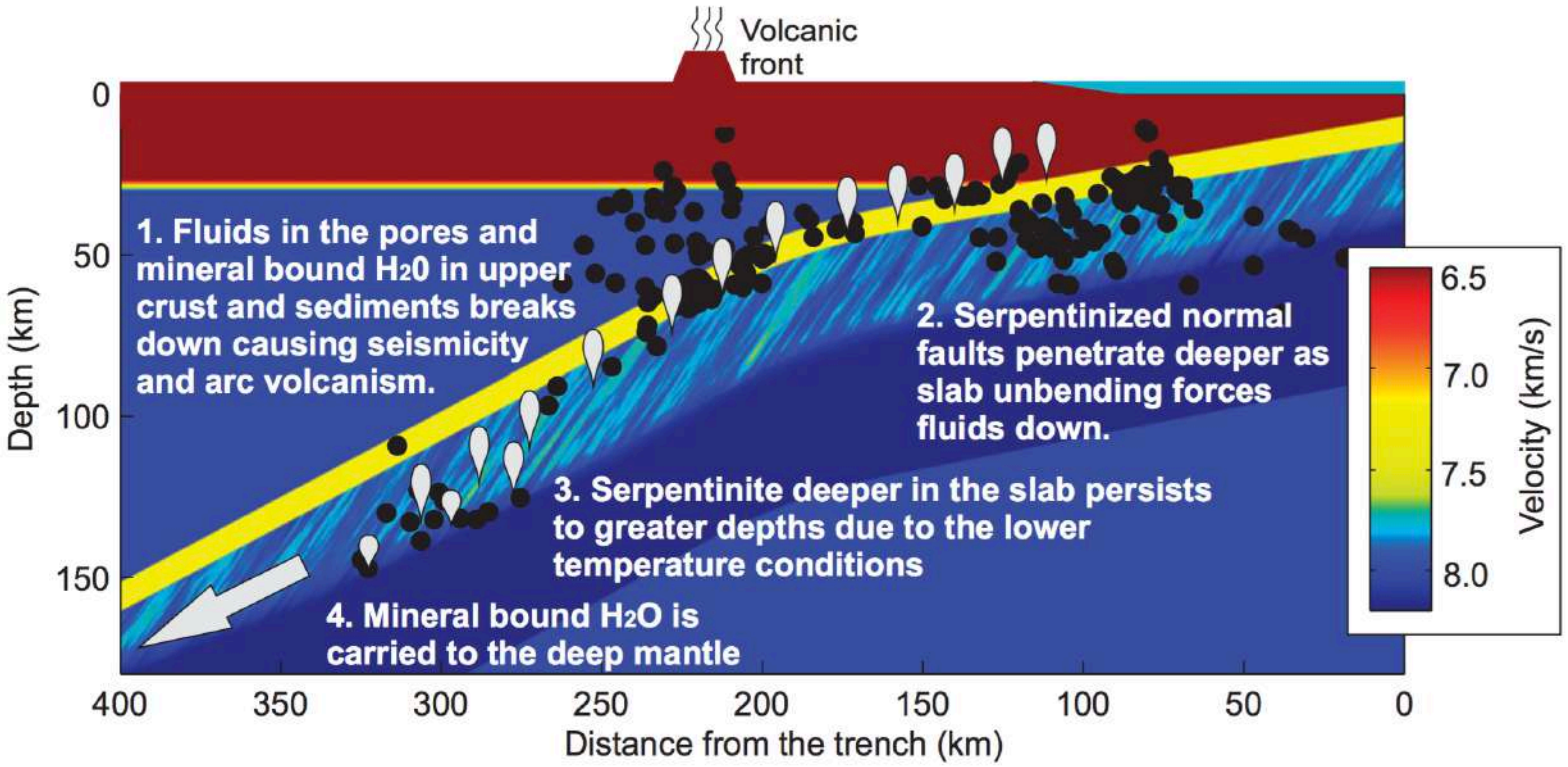

Japan 130Ma old slab: 17-31% serpentinization ➔ 2.0 – 3.5% H_2O

Garth&Rietbrock (2014a)

Northern Chile: “young” slab (45 Ma)

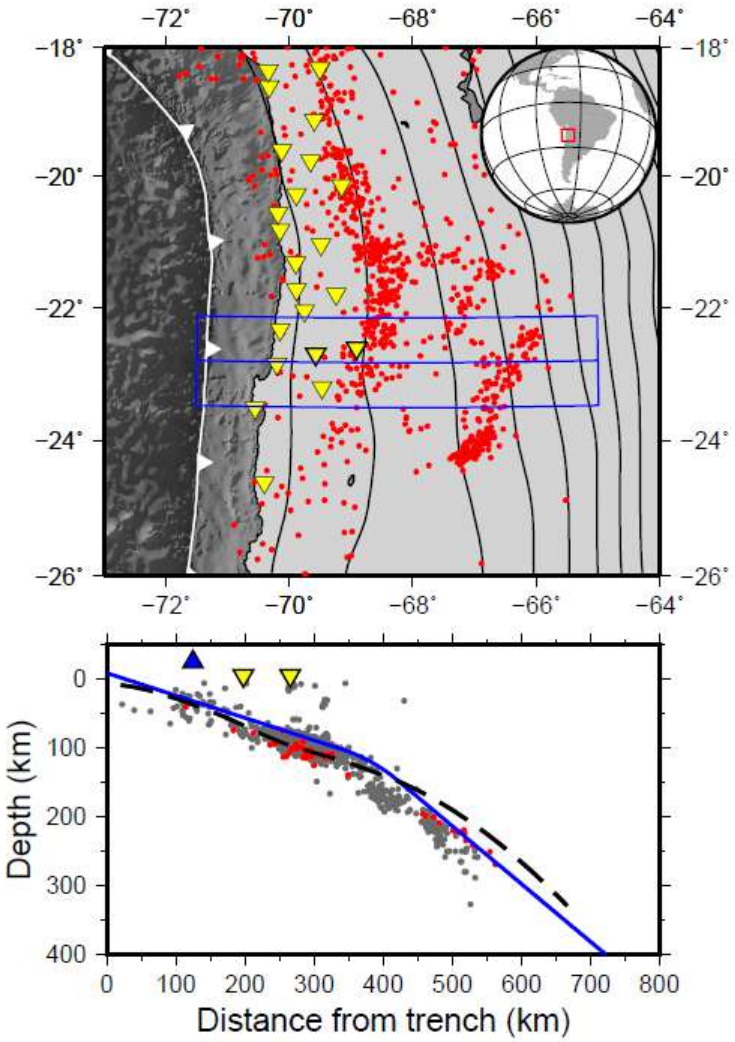

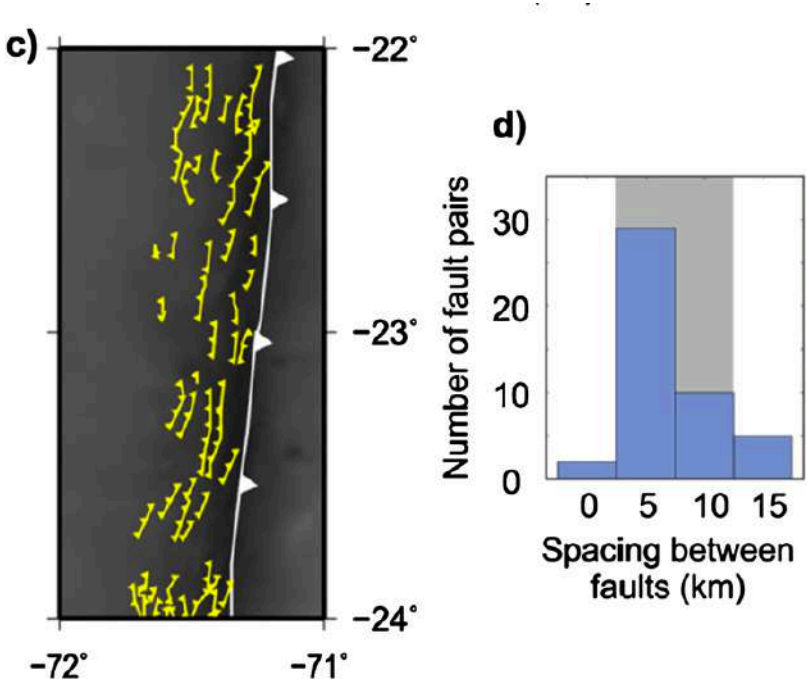

Garth&Rietbrock (2017)

Northern Chile: “young” slab (43Ma)

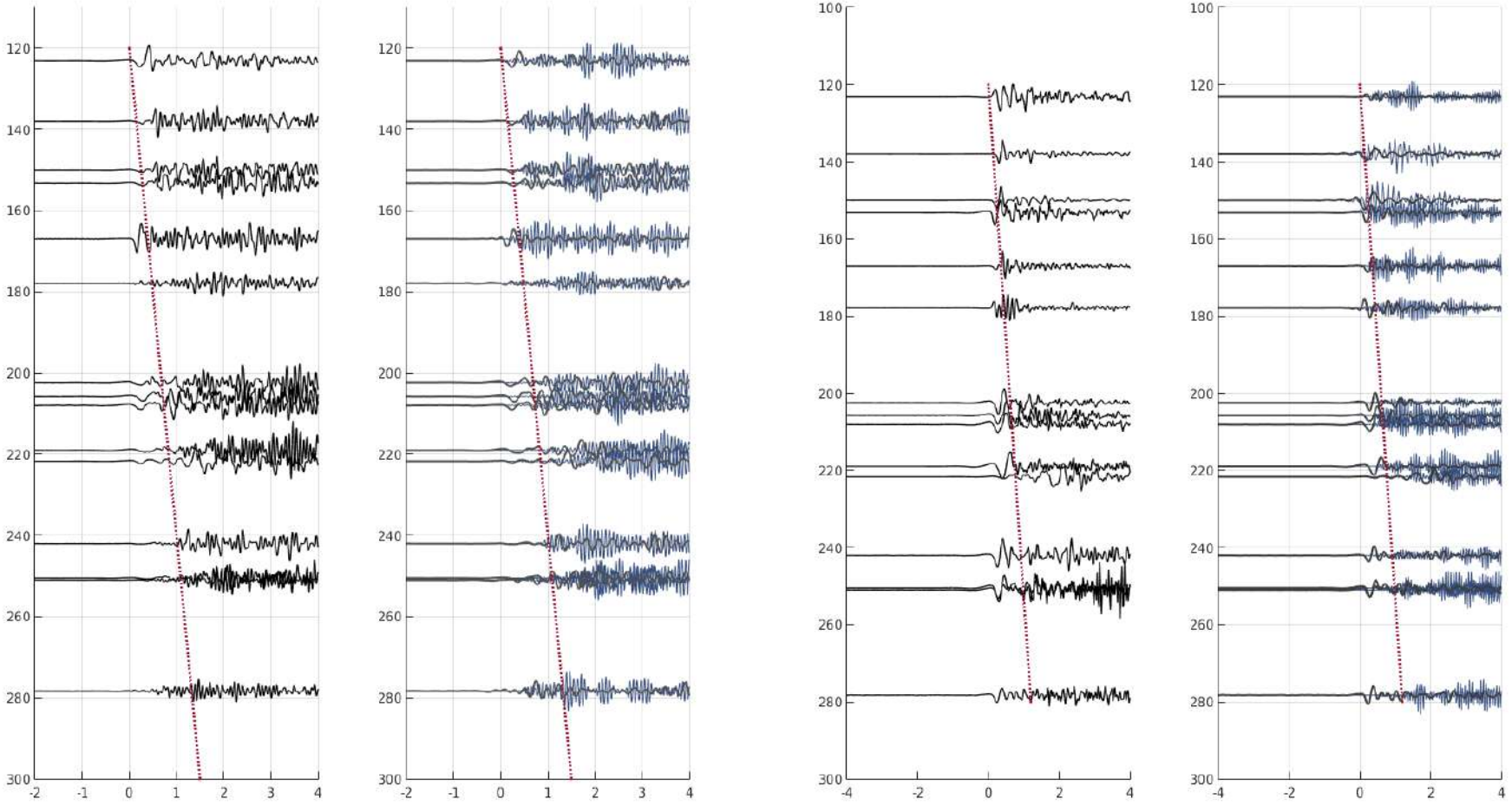

PB06

LVC

Garth&Rietbrock (2017)

Propagating wavefield: Long interaction with the slab!

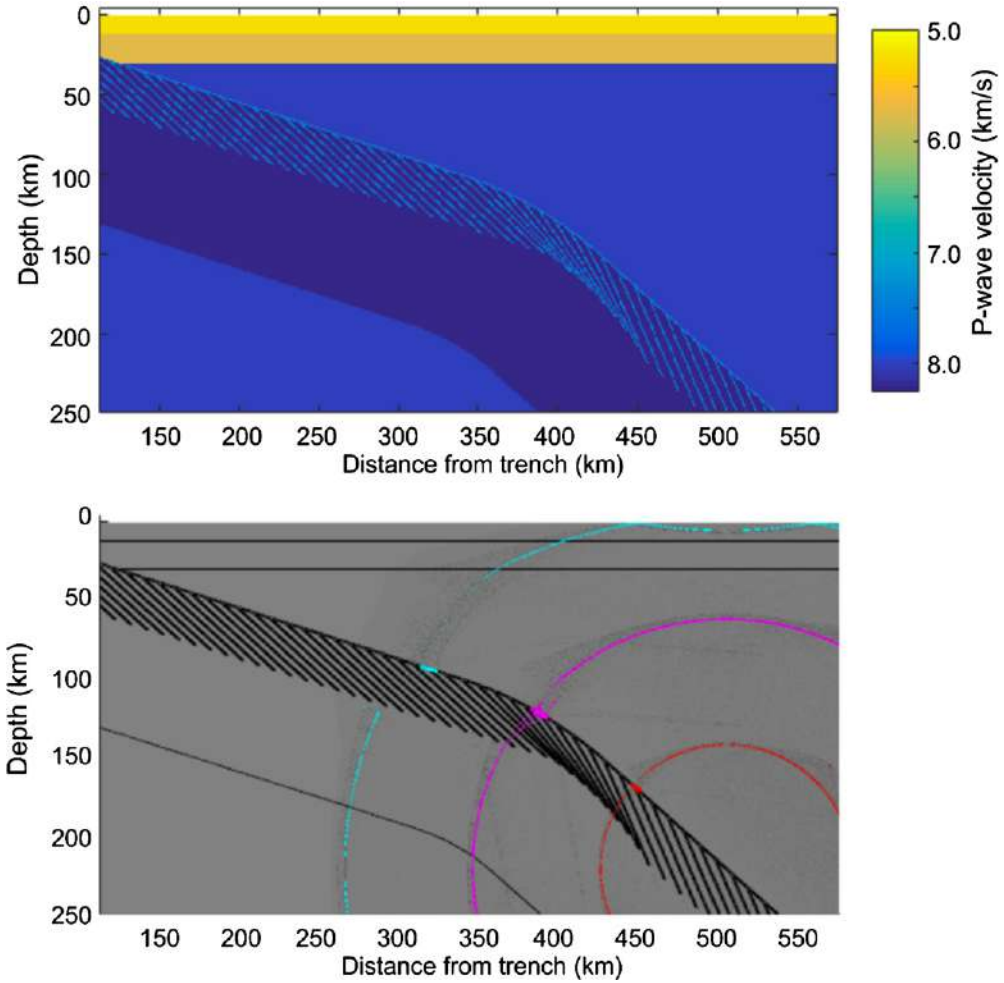

Garth&Rietbrock (2017)

LVZ & Hydrated faults are needed to model waveforms in Northern Chile

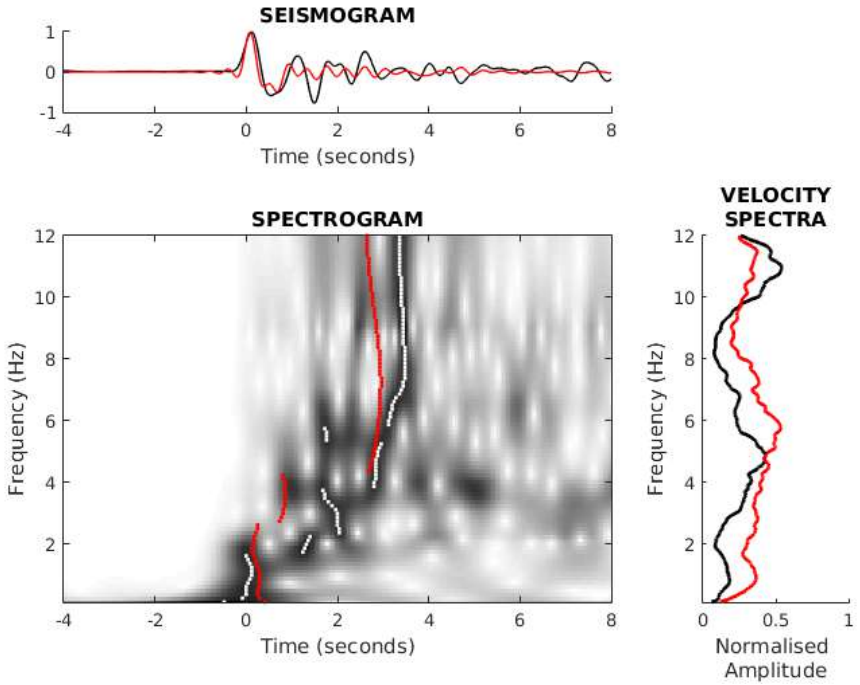

PB06

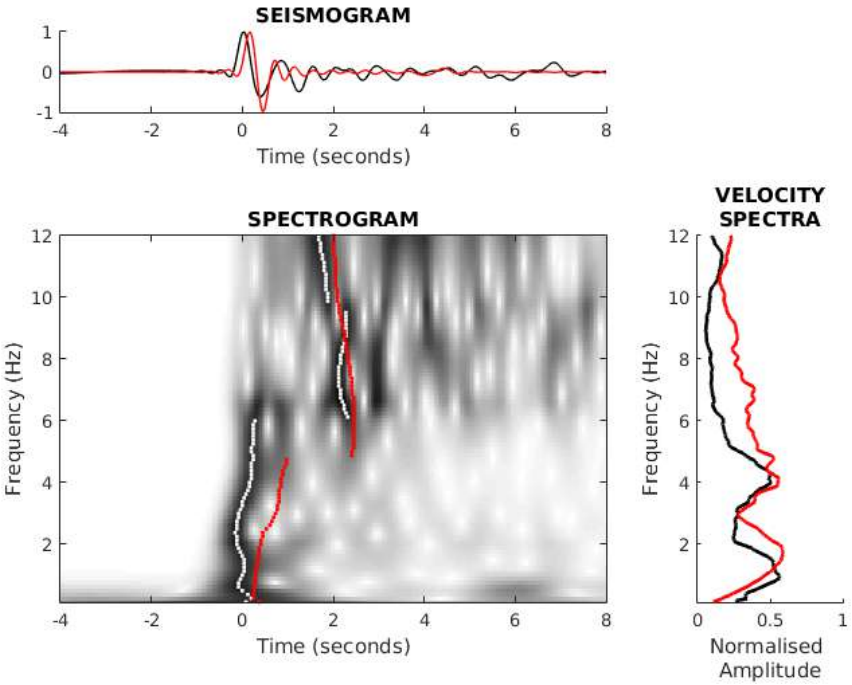

PVC

Garth&Rietbrock (2017)

Best fitting parameters

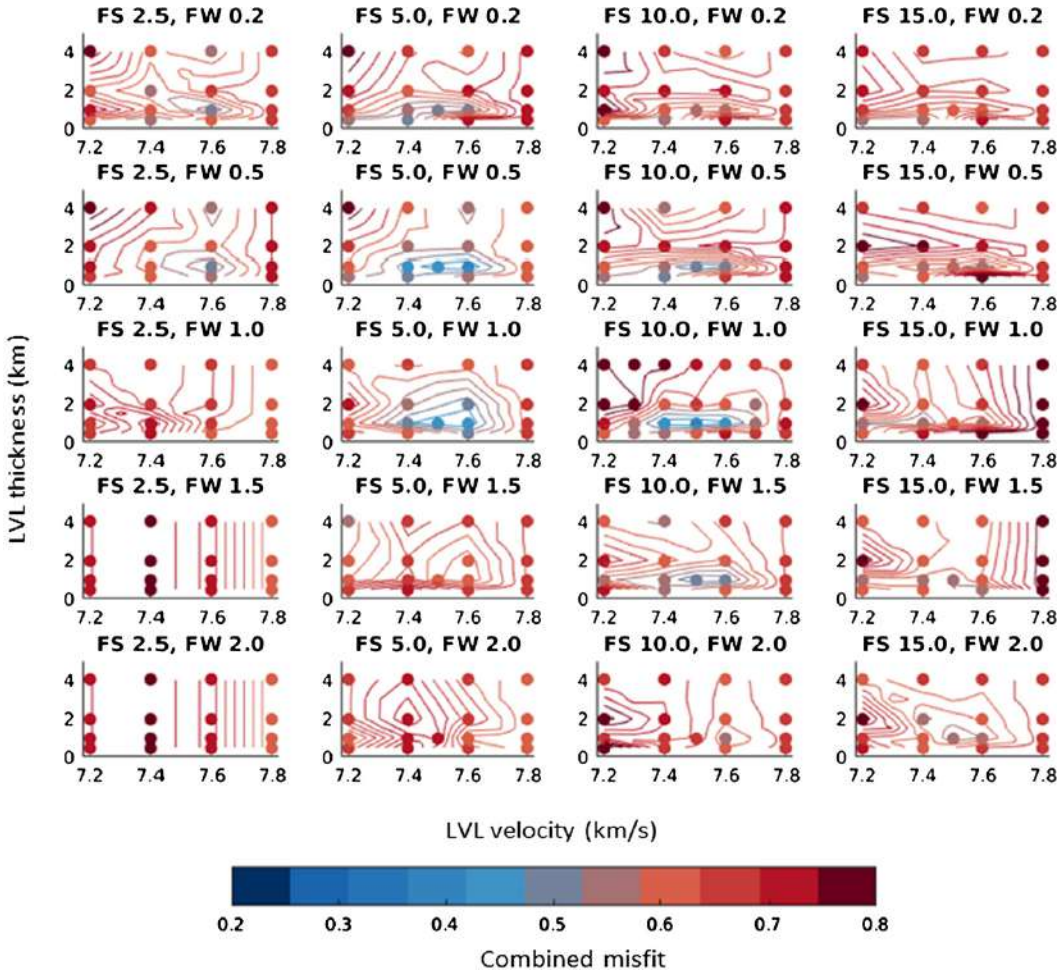

- LVL velocity
- LVL thickness
- Fault zone spacing
- Fault zone width

Central Andes 45Ma old slab: 5-15% serpentinized

Garth&Rietbrock (2017)

Consequences

Northern Japan (130Ma, 8km width)

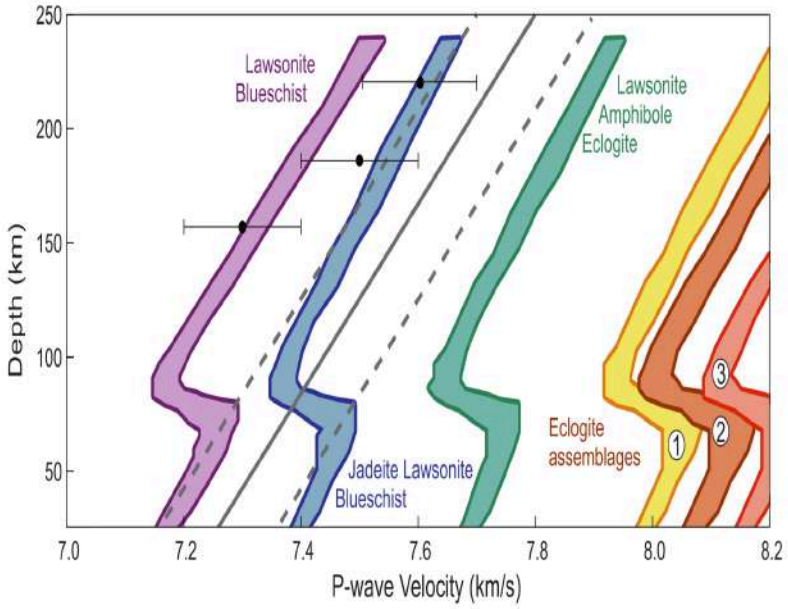

Northern Chile (45Ma), 2km width

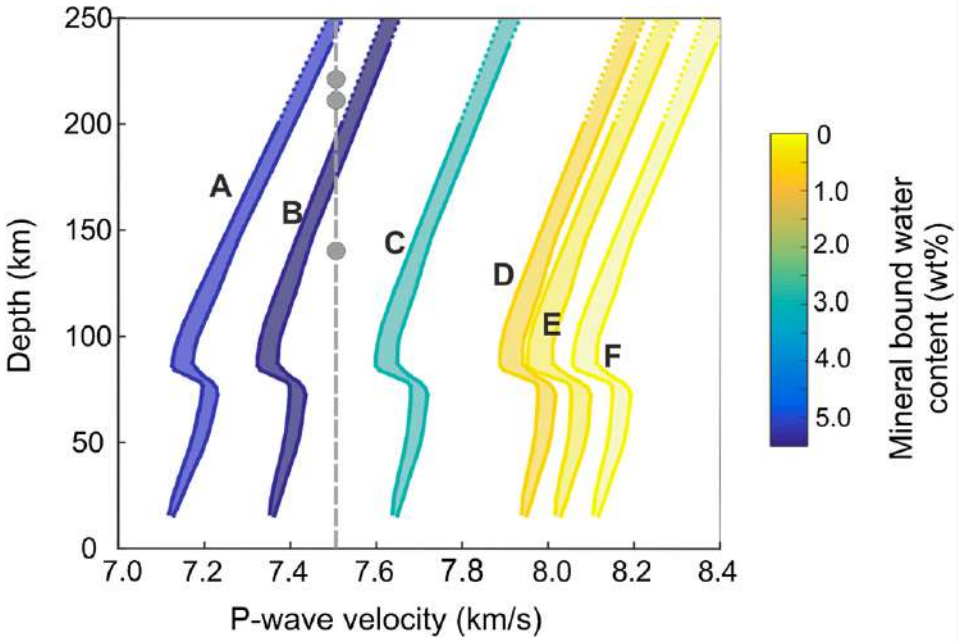

Bound in hydrated faults in the mental (bend faults)

170–318 Tg/M.y

13-42 Tg/M.y

Garth&Rietbrock (2014a,b)

Garth&Rietbrock (2017)

Conclusions

1. **Crustal low velocity layer: Metastability is needed !**
2. **Serpentinised faults in the mantel are the main source of water input deeper into the mantle**
3. **Approach also works for Alaska: Coulson et al. 2018**